

This discussion paper is/has been under review for the journal The Cryosphere (TC).
Please refer to the corresponding final paper in TC if available.

Variability of mass changes at basin scale for Greenland and Antarctica

V. R. Barletta, L. S. Sørensen, and R. Forsberg

Geodynamics Department, DTU Space, Elektrovej 2800 Kgs. Lyngby, Denmark

Received: 19 July 2012 – Accepted: 25 July 2012 – Published: 15 August 2012

Correspondence to: V. R. Barletta (vr.barletta@gmail.com)

Published by Copernicus Publications on behalf of the European Geosciences Union.

TCD

6, 3397–3446, 2012

Variability of mass changes

V. R. Barletta et al.

Title Page

Abstract

Introduction

Conclusions

References

Tables

Figures

◀

▶

◀

▶

Back

Close

Full Screen / Esc

Printer-friendly Version

Interactive Discussion



Abstract

During the last decade, the GRACE mission has provided valuable data for determining the mass changes of the Greenland and Antarctic ice sheets. Yet, discrepancies still exist in the published mass balance results, and analyses on the sources of errors and discrepancies are lacking. Here, we present monthly mass changes together with trends derived from GRACE data at basin scale for both the Greenland and Antarctica ice sheets and we assess, for the first time systematically, the variability and errors for each of the possible sources of discrepancies: mass inference methods, data sets and background models. We find a very good agreement between the monthly mass change results derived from two independent methods, which represents a cross validation. For the monthly solutions, we find that most of the variability is caused by the use of different data sets rather than different methods. Besides the well-known GIA trend uncertainty, we find that the degree-1 variability and the recent de-aliasing corrections have significant impact on monthly time series and trends respectively. We also show the remarkable differences between the use of release RL04 and the new RL05, and how the latter results in smaller mass trends for the majority of the basins. The overall variability of the solutions well exceeds the uncertainties propagated from the data errors and the leakage (as done in the past), hence we calculate new sound total errors for the monthly solutions and the trends. For the whole GRACE period our trend estimate for Greenland is $-234 \pm 20 \text{ Gt yr}^{-1}$ and $-83 \pm 36 \text{ Gt yr}^{-1}$ for Antarctica ($-111 \pm 15 \text{ Gt yr}^{-1}$ in the western part). These trends show a clear (with respect to our errors) increase of mass loss in the last four years.

1 Introduction

Determining reliably the mass balance (MB) of the large continental ice sheets is a major challenge. The results are of great societal importance, especially in terms of global sea level rise. The IPCC report of 2007 (Intergovernmental Panel on Climate Change,

TCD

6, 3397–3446, 2012

Variability of mass changes

V. R. Barletta et al.

Title Page

Abstract

Introduction

Conclusions

References

Tables

Figures

◀

▶

◀

▶

Back

Close

Full Screen / Esc

Printer-friendly Version

Interactive Discussion



2007) stated that the contribution from the ice sheets was insufficiently constrained, and since then a large effort has been done to improve the mass balance estimates, using different methods and data.

In 2005, Velicogna and Wahr (2005) showed for the first time the possibility of using data from the Gravity and Climate Recovery mission (GRACE) to determine the mass balance of the Greenland ice sheet. Since then many mass balance estimates of both Greenland and Antarctica have been published, both on ice sheet scale (Chen et al., 2006b; Ramillien et al., 2006; Forsberg and Reeh, 2007; Barletta et al., 2008; Velicogna, 2009) and drainage basin scale (Luthcke et al., 2006; Wouters et al., 2008; Schrama and Wouters, 2011; Sasgen et al., 2012).

The gravity changes observed by GRACE provide a direct measurement of the mass variations without the need of resorting to volume variations, avoiding some of the issues due to volume-mass conversion estimates. However, when using GRACE data to estimate continental mass balance, many corrections are applied either for hydrological purpose or for ice mass changes. The official processing centers remove some contributions like those due to tides, the atmosphere and the ocean. Other contributions have to be removed in a second stage in order to focus just on isolating the ice mass changes in selected regions. Each of these corrections is a potential source of variability in the mass balance computations. Glacial Isostatic Adjustment (GIA) has been recognized as the major cause of uncertainty in ice mass balance (Velicogna and Wahr, 2006; Barletta et al., 2008), especially in Antarctica. GIA is the solid Earth phenomenon responsible for the mantle flow from the equatorial region towards the Pleistocene deglaciated areas. This mass flow within the Earth produces variations in topography and in gravity, and the latter is detected by GRACE as a positive mass trend, that, in many areas, cannot easily be distinguished from surface mass accumulation.

However, for mass balance estimates, other sources of variability exist, whose importance has sometimes been underestimated. One source of uncertainty is related to geocenter motion (Chambers, 2006), and the different ways to infer it. Large mass

Variability of mass changes

V. R. Barletta et al.

Title Page

Abstract

Introduction

Conclusions

References

Tables

Figures

◀

▶

◀

▶

Back

Close

Full Screen / Esc

Printer-friendly Version

Interactive Discussion



Variability of mass changes

V. R. Barletta et al.

Title Page

Abstract

Introduction

Conclusions

References

Tables

Figures

◀

▶

◀

▶

Back

Close

Full Screen / Esc

Printer-friendly Version

Interactive Discussion



variations, like the ice melting in Greenland and Antarctica, generate not only gravity changes but also Earth surface displacements. This translates into a displacement of the center of mass (CM) with respect to the geometric center of the Earth, CF (Center of Figure): this movement is known as the geocenter motion. Therefore, mass balance estimates should take into account carefully the geocenter motion. However, since the GRACE satellites move together with the center of mass (CM) of the Earth, they cannot detect the geocenter motion, so this effect has to be recovered by other means. The correction for geocenter motion is still an open issue: there are different ways to calculate it and therefore more than one possible correction exist (Wu et al., 2012), and this can be a source of variability in mass balance.

Another source of variability in mass balance computation arises from different strategies for processing the raw data by the official centers, thus discrepancy between different solutions of GRACE data are known (Steffen et al., 2010; Barletta et al., 2012a). In this study we focus on the two official and most commonly used data sets and present the methodology we developed for analyzing different solutions, and deriving a quantitative estimate of the uncertainty due to the use of different solutions. Moreover, since the official GRACE processing centers have recently published a new release (RL05) of the monthly time series (though shorter and still incomplete), we have the opportunity to get an interesting overview of the difference between the RL04 and the new RL05 release, to our knowledge one of the first appearing in the scientific literature.

Different approaches in extracting the mass balance from GRACE level 2 data can be another source of variability and uncertainties. Velicogna and Wahr (2005); Luthcke et al. (2006); Schrama and Wouters (2011); Horwath and Dietrich (2009), and Sørensen and Forsberg (2010), all use different methods and this could be part of the reason of the wide variability in the results obtained in literature since 2005. In principle, independent methods should produce the same results if a careful calibration and cross validation has been carried out.

Variability of mass changes

V. R. Barletta et al.

[Title Page](#)[Abstract](#)[Introduction](#)[Conclusions](#)[References](#)[Tables](#)[Figures](#)[◀](#)[▶](#)[◀](#)[▶](#)[Back](#)[Close](#)[Full Screen / Esc](#)[Printer-friendly Version](#)[Interactive Discussion](#)

As a comprehensive result we provide up-to-date estimates of the monthly mass changes at basin scale for the Greenland and Antarctic ice sheets, and we also provide the net mass balance (the secular trend) for the time period considered. For each of these products, we also provide a sound error estimate that takes into account most of the potential source of uncertainties, beside the data error. In particular, we estimate the contribution to the error budget due to GIA corrections, to the treatment of the geocenter correction, to the choice of different data source, and to different post-processing methods. This last step allows also to compare and cross-validate two independent radically different approaches to mass balance estimates from GRACE data.

2 Data and corrections

We aim at deriving estimates of the uncertainties in the mass balance from GRACE at basin scale for Antarctica and Greenland, taking into account a variety of potential sources of uncertainties, some of which have been sometimes overlooked. In this section, we briefly discuss each of these sources of variability, in more detail.

2.1 GRACE L2 data releases

GRACE data are processed and provided to the scientific community by two official processing centers: Centre for Space Research, University of Texas (CSR), GeoForschungsZentrum, Potsdam (GFZ), with the Jet Propulsion Laboratory, California (JPL) providing the so-called validation solutions. Other research institutes such as the Centre National d'Etudes Spatiales (CNES) and Institut für Geodäsie und Geoinformation, University of Bonn also provide GRACE products. The different solutions are of similar quality, but are not identical because of different processing strategies.

The processing centers provide GRACE level-2 (L2) data, which consist of monthly GRACE solutions or models, i.e. sets of fully normalized spherical harmonic coefficients, called Stokes coefficients. The analysis of the present work is based on the

monthly GRACE L2 release 4 (RL04) and 5 (RL05) gravity field models provided by CSR (Bettadpur, 2007) and GFZ (Flechtner, 2007a). CSR and GFZ provide both formal and calibrated error estimates on the Stokes coefficients with their models, with the exception of CSR RL05 which at the moment do not include calibrated errors. This study is based on 113 CSR RL04, 105 GFZ RL04, 84 CSR RL05 and 72 GFZ RL05 monthly models, within the time span April 2002–February 2012.

The low degree harmonic coefficients provided in the level-2 RL04 require some attention. The C_{20} values show anomalous variability. Therefore, we replace these GRACE C_{20} coefficients with estimates derived from satellite laser ranging (SLR) (Cheng and Tapley, 2004). In the RL04 models, we also restore the C_{20} , C_{21} , S_{21} , C_{30} , and C_{40} coefficients with the reference values of secular changes reported in the level-2 Processing Standards Document (Bettadpur, 2007).

GRACE data from all the processing centers are corrected at an early stage for atmospheric variability and ocean bottom pressure (OBP) fields. In the processing used to derive the new RL05, many improvements have been implemented compared to RL04 (Dahle et al., 2012a,b; Bettadpur et al., 2012). Some examples of these improvements are significant upgrades to the background gravity Model (GIF48), the GPS constellation being homogeneously reprocessed improved the determination of GRACE satellites orbits, the ocean tide model and the model for planetary ephemerides were changed and accelerometer biases estimated are improved. As a consequence, for example, the low degree coefficients do not need to be restored when using RL05, and degree 2 does not have to be replaced with the one coming from SLR. In addition new atmosphere and ocean models have been used to correct the data. An overall visible result is a small decrease of noise especially the “stripes”.

2.2 GAC correction

The gravity field generated by atmosphere and ocean is computed from 6-hourly pressure field, which is the output of the respective models. These 6-hourly simulated gravity fields are called Atmosphere and Ocean de-aliasing products (AOD1B) and are used

Variability of mass changes

V. R. Barletta et al.

Title Page

Abstract

Introduction

Conclusions

References

Tables

Figures

◀

▶

◀

▶

Back

Close

Full Screen / Esc

Printer-friendly Version

Interactive Discussion



locally to correct the gravity field along the track of the satellites. This product is based on a combination of the ECMWF (European Center for Medium Weather Forecast) operational atmospheric fields and the baroclinic ocean model OMCT (Ocean Model for Circulation and Tides) (Flechtner, 2007b). After the processing, the monthly average of Atmosphere and Ocean gravity models is generated as a collateral product of GRACE data, and it is called GAC.

The AOD1B RL05 is based on an ocean model with increased vertical and horizontal resolution and updated parameterization. AOD1B RL05 does not have some of the coastal artifacts that were present in the AOD1B RL04 (Bettadpur et al., 2012). As soon as the new RL05 was released, it was possible to compare the GAC products of RL04 and RL05 and the difference is clearly visible (see Fig. 1). With respect to GAC-RL05, the GAC-RL04 time series shows a sudden jump in 2009 at some locations in the ocean, especially close to the coast of Antarctica (Fig. 1). The jump is artificial and is caused by an offset in the atmospheric pressure fields that are used to force the ocean model (H. Dobslaw, personal communication, 2012).

This jump affects the monthly mass change estimate in some basins. We derive a correction for RL04 data which remove the jump in 2009 and the trends. One simple way is to use the differences between the monthly GAC-RL05 and GAC-RL04 models that we call GAC[04–05], for the common months. However, this shortens our RL04 time series to that of RL05 (January 2004–December 2010). We use this correction when comparing the RL04 and RL05 time series, but in our final estimate, in order to use the full length of the RL04, we use another correction $M_{\text{GAC}}(t)$ which is derived by fitting a function (step wise plus a linear term) to the monthly GAC[04–05], for each basin. We also derived the $M_{\text{GAC}}(t)$ standard deviation with respect to the GAC[04–05] and use it as monthly error. Moreover, we compute the contribution of the $M_{\text{GAC}}(t)$ correction to the trend.

Variability of mass changes

V. R. Barletta et al.

Title Page

Abstract

Introduction

Conclusions

References

Tables

Figures

◀

▶

◀

▶

Back

Close

Full Screen / Esc

Printer-friendly Version

Interactive Discussion



2.3 Degree-1

The geocenter motion, in harmonic coefficients, is represented by the degree-1 (C_{10} , C_{11} , and S_{11}) components. These are only partially detected by GRACE, but they need to be included in the mass derived by GRACE (Chambers, 2006). Neglecting the degree-1 would lead to a systematic error in mass variations, especially for Antarctica.

The correction for the degree-1 is still an open issue, and it is subject to much debate. In the GRACE official web site (NASA GRACE Tellus <http://grace.jpl.nasa.gov>) the degree-1 is that from Swenson et al. (2008). However, many other geocenter motion time series are available, calculated for GRACE and for other purposes (Wu et al., 2012). Those geocenter monthly time series differ in both amplitude and phase. It is also important to take into account whether a given time series includes the GIA degree-1 trend or not. For instance, Swenson et al. (2008) already has the GIA degree-1 term included (based on ICE5g-VM2 GIA model), while the SRL derived degree-1 estimates (Cheng et al., 2010) are not corrected for GIA.

The SLR derived geocenter motion is reported to be the most precise (Wu et al., 2012), however degree-1 derived from *GRACE and ocean models* (Swenson et al., 2008; Riva et al., 2012) or *GRACE and GPS* (Rietbroek et al., 2012a) have a smaller amplitude than the one based on SLR. Klemann and Martinec (2009) show the large variability of GIA degree-1 trends with respect to the viscosity of the lower mantle. Since one of the main problems for Antarctica is that GIA is poorly constrained there (both for the ice history and for viscosity model), we are left with a very wide choice of possible degree-1 time series which also contribute to the variability of our estimated monthly mass changes as well as their trends.

To deal with this issue, we build a sensitivity kernel for the degree-1 contribution at basin scale, i.e. we estimate the mass variation in Gt for 1 mm of variation in each of the X , Y , and Z components of the geocenter motion. For each basin, the degree-1 correction, in terms of mass change for each component (X, Y, Z), is obtained by multiplying the sensitivity kernel (Tables 1 and 2) by the X , Y , and Z geocenter time

TCD

6, 3397–3446, 2012

Variability of mass changes

V. R. Barletta et al.

Title Page

Abstract

Introduction

Conclusions

References

Tables

Figures

◀

▶

◀

▶

Back

Close

Full Screen / Esc

Printer-friendly Version

Interactive Discussion



series (in mm) or their trends (in mm yr^{-1}). The total degree-1 correction is the sum of the three components.

In the present work we use three independent degree-1 time series:

1. Swenson et al. (2008), for seasonal and trend component (SW).
2. Rietbroek et al. (2012a), just for the seasonal component (not for the trend), (RR).
3. SLR – Cheng et al. (2010), for the seasonal component, and for the trend we will apply a GIA correction (Klemann and Martinec, 2009), (SLR).

These are among the most up-to-date time series, each of them representing a different method to infer the degree-1.

For the geocenter motion monthly solution we compute the monthly average with its standard deviation between the three detrended time series (SW, RR and SLR). We use this average and the degree-1 sensitivity kernel to compute our preferred degree-1 correction in mass balance time series (for each basin).

For geocenter motion trend we use an average (with its standard deviation) between four trends as in Table 3. The first (first line of the Table 3) is the trend extracted from the Swenson et al. (2008) time series. The second (second line of the Table 3) is the trend reported in Rietbroek et al. (2012b). The third and fourth trend (third and fourth lines) is a combination between the trend extracted from SLR – Cheng et al. (2010) time series minus two GIA geocenter motion valid alternatives: one is given in Wu et al. (2012) for ICE5g/IJ05/VM2 ($X = -0.12$, $Y = 0.24$, $Z = -0.48$) the other in Klemann and Martinec (2009) ($X = -0.13$, $Y = 0.33$, $Z = -0.80$).

2.4 De-stripping and filtering GRACE data

The GRACE monthly models are known to be affected by both noise (instrumental and statistical) and peculiar features in form of north-south oriented stripes (Swenson and Wahr, 2006). The latter are due to systematic errors related to orbital trajectories and

Variability of mass changes

V. R. Barletta et al.

Title Page

Abstract

Introduction

Conclusions

References

Tables

Figures

◀

▶

◀

▶

Back

Close

Full Screen / Esc

Printer-friendly Version

Interactive Discussion



data processing strategies, and are apparent as spurious spatial correlations (Kusche et al., 2009).

We apply the de-stripping method presented in Kusche et al. (2009) to the GRACE L2 solutions. This is a non-isotropic smoothing procedure, based on approximate de-correlation and successive regularization of the GRACE monthly solutions. The results provided here is obtained using a weak smoothing (smoothing parameter $a = 10^{12}$), i.e. using the DDK3 filtering method, which is available on the web site of GFZ (<http://icgem.gfz-potsdam.de/ICGEM/TimeSeries.html>). In particular the data DDK3-filtered we use corresponds to a resolution of 240–330 km. The effective filter has a wider radius in the E–W than N–S direction and at high latitudes, the anisotropic filtering kernel becomes close to isotropic.

Data filtering and de-stripping affect the mass balance at basin scale in different ways, depending on the method. However, in each of our methods, these effects are also effectively counteracted by a proper calibration which allows us to consider the variability due to filtering as a part of the method errors. This also holds for the data cutoff degree (i.e. the data resolution): for all the GRACE data releases employed in this study we use the harmonic coefficients up to degree 60 (max degree for CSR RL04), but in the calibration phase we also tested the differences resulting from using higher harmonic degrees when available.

2.5 Glacial isostatic adjustment

On the NASA GRACE Tellus site (<http://grace.jpl.nasa.gov/data/pgr>) a GIA model (Paulson et al., 2007) is provided. This model is recommended as the best model, and it is associated with a uniform uncertainty of $\pm 20\%$. This model is based on the global ICE-5g ice history of Peltier (2004), and a simplified VM2 Earth model: a 4-layered approximation to VM2 viscosity profile. This model also includes the rotational feedback based on the formulation of polar wander described by Mitrovica et al. (2005). Through the sea level feedback, the center-of-mass motion is also taken into account. For Antarctica, another GIA model is the IJ05 (Ivins and James, 2005) that has often

Variability of mass changes

V. R. Barletta et al.

Title Page

Abstract

Introduction

Conclusions

References

Tables

Figures

◀

▶

◀

▶

Back

Close

Full Screen / Esc

Printer-friendly Version

Interactive Discussion



been employed as a correction in mass balance studies (Horwath and Dietrich, 2009; Chen et al., 2006a; Gunter et al., 2008, 2009).

Thomas et al. (2011) show that traditional GIA models (ICE5g-VM2, IJ05) predict an uplift that is too large, when compared to the uplift rates measured by GPS, and they indicate that the Riva et al. (2009) empirical model is the one which gives the best fit. Riva et al. (2009) find a GIA pattern for Antarctica by combining GRACE and ICESat data, and they find a smaller signal than the one of traditional GIA models (ICE5g-VM2, IJ05). Wu et al. (2010) also find a GIA pattern empirically by performing a global inversion with GRACE data, and the signal over Antarctica is smaller than ICE5g but higher than Riva et al. (2009). So there are now many indications that traditional GIA models overestimate GIA signal over Antarctica and for this reason much work has been done in the last years taking into account newly available data to constrain the LGM (Last Glacial Maximum) ice models. However, these new ice models are still not publicly available, hence using the available traditional LGM ice models we derive revised proper GIA corrections, after new considerations, and we use them together with the Riva et al. (2009) empirical GIA model.

One reason of the GIA overestimate can be the excess of ice melting during the LGM for the traditional ice models (ICE5g, IJ05) which clearly violates the geological evidence on the ice history (Todd et al., 2010; Ackert et al., 2011; Mackintosh et al., 2011). However due to the trade-off between ice-history and solid Earth response in GIA, another way to predict a smaller signal in Antarctica is to choose a lower viscosity profile, especially in the western part where the majority of the deglaciation took place. Barletta et al. (2008) shows that for low viscosities, the GIA corrections are smaller. In fact with respect to traditional viscosity profiles, like VM2 Peltier (2004), lower viscosities produce faster relaxation so that most of the mantle flow nowadays is over. For now there are no new ice models available, so we propose two alternatives, using two traditional ice models with low viscosity profile.

We also tested the empirical GIA pattern extracted in Barletta and Bordoni (2009) and we verified that it produces mass balances similar to those produced by

TCO

6, 3397–3446, 2012

Variability of mass changes

V. R. Barletta et al.

Title Page

Abstract

Introduction

Conclusions

References

Tables

Figures

◀

▶

◀

▶

Back

Close

Full Screen / Esc

Printer-friendly Version

Interactive Discussion



ICE5g-VM2. The GIA pattern obtained in that work was an upper bound of possible GIA patterns (the positive signal due to GIA was not distinguished from others due to possible present day mass accumulation). So we decided to use ICE5g-VM2 as an upper bound of the GIA contribution.

In Greenland the GIA signal is small with respect to the total trend but, depending on the model, it is not negligible. For this region two commonly used models, ICE5g and ANU model (Fleming and Lambeck, 2004), especially for some basins, predict signals with opposite sign. We use both these two model because the difference between them ensure a reliable confidence interval for GIA prediction in Greenland.

GIA corrections are based on 5 layered incompressible Earth models without lateral heterogeneities. We compute the solid Earth Green's functions (Love numbers) according to the analytical approach described in the benchmark of Spada et al. (2011) with the benchmarked code TABOO (Spada et al., 2004). The sea level equation is solved self-consistently with the pseudo-spectral approach (Mitrovica and Peltier, 1991) implemented in the optimized code TSec01 developed for Barletta and Spada (2011, 2012b) and benchmarked in Spada et al. (2012). We include the degree-1 and perform the computations in the center of mass (CM) reference, up to degree 128, without rotational feedback.

To summarize, we apply five different GIA corrections:

1. The revised version of Paulson et al. (2007) ICE5g-VM2 GIA model, which uses a compressible fully layered Earth model (Geruo A/Paulson). This model is used for both Antarctica and Greenland.
2. The ANU model for Greenland (Fleming and Lambeck, 2004).
3. The Riva09 empirical GIA fingerprint for Antarctica (Riva et al., 2009)
4. ICE5g-LV with a low viscosity for Antarctica
5. IJ05-LV with a low viscosity for Antarctica

Variability of mass changes

V. R. Barletta et al.

Title Page

Abstract

Introduction

Conclusions

References

Tables

Figures

◀

▶

◀

▶

Back

Close

Full Screen / Esc

Printer-friendly Version

Interactive Discussion



Variability of mass changes

V. R. Barletta et al.

[Title Page](#)[Abstract](#)[Introduction](#)[Conclusions](#)[References](#)[Tables](#)[Figures](#)[I◀](#)[▶I](#)[◀](#)[▶](#)[Back](#)[Close](#)[Full Screen / Esc](#)[Printer-friendly Version](#)[Interactive Discussion](#)

By varying, within a chosen range, the lithospheric thickness and the viscosity of the upper and lower mantle we compute several corrections. Then we compute the average and the standard deviation for each of the ensemble Ice+Earth model, the 2, 4 and 5 in the list above. The Earth parameters ranges for lithospheric thickness (LT), upper (UMV) and lower (LMV) mantle viscosities are

(a) for ANU: LT = 50 to 100 km, UMV = 2 to 5×10^{20} , LMV = 0.5 to 2×10^{22} Pa s

(b) for ICE5g-LV: LT = 75 to 120 km, UMV = 0.1 to 0.2×10^{20} and LMV = 0.15 to 0.2×10^{22} Pa s

(c) for IJ05-LV: LT = 65 to 115 km, UMV = 0.1 to 0.2×10^{20} and LMV = 0.1 to 0.2×10^{22} Pa s.

Due to the short time scale considered here, the GIA correction only affects the linear trend, and not the month-to-month behavior of the time series. We estimate the uncertainties for all these proposed models by different approaches: the GIA uncertainties for ICE5g-VM2 are computed as in Barletta and Spada (2011, 2012b); the Riva09 model is provided with error estimates, and we propagate these to obtain error estimates of the final mass changes.

In our final preferred trend we use as GIA uncertainties the maximum on GIA uncertainties among the four models. Tables 4 and 5 report the values used in this study.

3 Methodology

Two different and independent methods that use the same input data should ideally lead to the same results. For gravity-derived mass changes the major difference between one method and another is the leakage treatment. In fact with low resolution measurements (such as GRACE), discriminating the signal coming from inside the region of interest from the one coming from outside is a challenging problem. By assuming that the region of interest produces a much stronger signal than the surrounding,

many methods treat the leakage by enlarging the integration areas (or the averaging kernel). Horwath and Dietrich (2009) deal with this problem in quite a systematic way and show the errors in mass changes associated with leakage. However the leakage treatment is embedded in the method so, together with filtering (and de-stripping), after suitable calibration it becomes effectively part of the “method errors”. The two methods that we use, are different and independent and treat the leakage problem in different ways.

3.1 Method 1: mass inversion

The direct point mass inversion method used for determining the monthly mass changes from the monthly GRACE data is based on Forsberg and Reeh (2007) and Sørensen and Forsberg (2010). Prior to the inversion, corrections and filtering are applied to the GRACE data as described in the previous section. The elastic response of the solid Earth to present-day ice mass changes, involves changes in the gravity field. This must be removed from the GRACE data, before deriving the surface mass changes from the observed gravity changes.

The elastic corrections based on the model of Farrel (1972), as also presented by Wahr et al. (1998), are used to make “reduced” gravity disturbances for the observation equations in the inversion. The inversion is performed on a set of N_y observations $\underline{y} = \{\delta g_k\}$, $k = 1 \dots N_y$, i.e. gravity disturbances at the altitude of the satellites, and solved for a point-like mass ensemble $\underline{x} = \{m_j\}$, $j = 1 \dots N_x$ located at coordinates (θ_j, ϕ_j) which define the solution area. The linear problem $\underline{y} = \mathbf{A}\underline{x}$ is solved using a generalized Tychonov inverse approach $\underline{x} = (\mathbf{A}^T \mathbf{A} + \lambda \mathbf{I})^{-1} \mathbf{A}^T \underline{y}$, where λ is a smoothing parameter and the observation matrix \mathbf{A} is built upon the attraction of a point mass of the sphere to the measured gravitational attraction at the orbit level by

$$\delta g_k = G m_j a^2 \frac{(h + a) - a \cos \psi_{kj}}{r_{kj}^3}.$$

Variability of mass changes

V. R. Barletta et al.

Title Page

Abstract

Introduction

Conclusions

References

Tables

Figures

◀

▶

◀

▶

Back

Close

Full Screen / Esc

Printer-friendly Version

Interactive Discussion



Here G is the gravity Newton constant, a is the mean radius of the Earth, h is the height of the observation, r_{kj} and ψ_{kj} are the distance and the angle, respectively, between the observation δg_k and the solution point m_j .

The inversion method has been refined, optimized and calibrated for this work. First we optimized the solution area using an icosahedron-based grids (Tegmark, 1996) with disk elements of almost equal area. Then we improved and calibrated the solution area in order to reduce as much as possible the leakage from signal outside the region of interest. The inversion method assume that the gravity signal is negligible outside the region of interest, otherwise such a signal would be forced to be part of the ice mass changes in the solution area. Once this assumption is verified by applying the method on synthetic data, we find that it is able to recover up to 99 % of the mass. One strategy for mitigating the effect of ocean mass changes being erroneously modelled as ice sheet changes is to force the ocean signal to be zero, especially in the far field. The signal outside the region of interest that is farther than some hundreds km (300 to 500) from the boundary of the solution area can be forced to zero (Zero Mask) without compromising the signal of interest. Another strategy is to build a Complementary Solution Area (CSA) around the primary one. The CSA is a belt around the original solution area, but separated by a gap of some hundreds of km (300 to 500) and it accounts for the signal outside the original solution area. We used a combination of the two above strategies, and we calibrated the gap for CSA and the distance for the Zero Mask. The parameters we chose with the calibration allow us to retrieve up to 98 % of different kind of synthetic signals. The regularization parameter (the smoothing parameter λ) used for this study was also chosen after calibration using a synthetic data set.

Figure 2a shows the solution area for the inversion of the trend over Antarctica. Figure 2b shows the solution area for the inversion of the trend over and around Greenland, and the point-like mass units, used as solution area for the inversion, are also visible. The closest surrounding ice-covered areas (Ellesmere Island) are included, to reduce leakage. In fact Ellesmere Island has a strong trend and it is so close to the

Variability of mass changes

V. R. Barletta et al.

[Title Page](#)[Abstract](#)[Introduction](#)[Conclusions](#)[References](#)[Tables](#)[Figures](#)[◀](#)[▶](#)[◀](#)[▶](#)[Back](#)[Close](#)[Full Screen / Esc](#)[Printer-friendly Version](#)[Interactive Discussion](#)

North West Greenland, that it cannot be treated as the rest of the surrounding sea and islands around Greenland.

Once we obtained a mass grid from the inversion scheme for each month we integrate over each basins area to derive the total mass change for Antarctica and Greenland. The mass estimates of each of the basins is a summation of the point mass changes within each basin mask definition (Sect. 3.3).

3.2 Method 2: conversion and integration

From the GRACE spherical harmonic coefficients, surface mass density in water equivalent (w.e.) is generated, as presented in Wahr et al. (1998). In order to take into account leakage, we integrate over a region more extended over the sea than the original area of interest, as done in Barletta et al. (2008). We use (for each basin) three integration areas which extend over the sea for 100, 200 and 300 km, and then we derive a weighted average of the three integrals. The largest weight is on the results obtained with the integration area which extend for 300 km from the coast, since this is the resolution of the data, and in this way we are able to reduce the leakage, and recover most of the signal.

This method is basically a simplified version of the Velicogna and Wahr (2005) and Horwath and Dietrich (2009) method, and it does not need a suitable averaging kernel nor a rescaling factor. The latter is usually used to retrieve the signal lost either for the filtering, the cutt-off degree (data resolution) and the leakage.

The leakage for this method is only considered coming from the land that we are analysing, so we do not get rid of the leakage coming from the ocean into the land.

3.3 Basin definitions and resolution

For the Greenland ice sheet we use the basin definition presented in Hardy et al. (2000). The Greenland ice sheet is divided into seven major basins, that are shown

Variability of mass changes

V. R. Barletta et al.

Title Page

Abstract

Introduction

Conclusions

References

Tables

Figures

◀

▶

◀

▶

Back

Close

Full Screen / Esc

Printer-friendly Version

Interactive Discussion



in Fig. 3a. The Antarctic ice sheet is divided into 27 major basins as shown in Fig. 3b, which is the same as Zwally et al. (2012).

Both methods use these basin definitions even if the sampling (their resolution and geometry) are performed on different grids and so the contour of each region is not exactly the same, especially for the smallest basins. The method 1 use an icosahedron-based grids with almost equal area disks of about 40 and 20 km radius for Antarctica and Greenland respectively (Fig. 2). The method 2 uses Gaussian grids of 128×256 cells (latitude \times longitude). Notice that GRACE resolution is about 300 km and both methods use grids with higher resolution for the mass reconstruction but the results depend strongly on data resolution and just slightly on the method resolution, i.e. the internal working resolution (and format) for each of the method.

3.4 Uncertainty estimates

As already mentioned, the mass estimates are associated with several sources of uncertainties. Some are coming from the data errors and others introduced through the algorithms employed, sampling grid sizes or smoothing and other parameters (in the inversion).

We derive the uncertainties which are related to the data errors provided directly with the GRACE monthly models, by using a Monte-Carlo like approach in which 100 simulations are performed. The simulations are created from Stokes coefficients drawn from normal distributions with zero mean, and the calibrated standard deviation provided with the GRACE level-2 data (Tscherning et al., 2001).

We deal with both precision and accuracy errors in our final results. The precision error accounts for the statistically distributed random error around one average values. The accuracy error accounts for how much the expected value deviates from the “true” value.

For the precision error we provide the 95 % confidence interval (2σ) propagated from the data. For each method, by using synthetic data (as in the calibration procedure) we assess its accuracy so that it can be added to the precision error to give the total error.

Variability of mass changes

V. R. Barletta et al.

Title Page

Abstract

Introduction

Conclusions

References

Tables

Figures

◀

▶

◀

▶

Back

Close

Full Screen / Esc

Printer-friendly Version

Interactive Discussion



We find that the accuracy error related to the methods alone is about 2% which is much smaller than the difference found by the use of different datasets. So in our final estimates we neglect this small contribution, and our accuracy error is derived from the difference coming from the use of different methods and dataset.

3.5 Best estimate and comparison strategies

The strategy to deal with many possible combinations of data, methods and corrections is relevant on one side to minimize the number of steps and so the possible sources of (human) mistakes, and on the other to make the procedure clearer and so easier to be verified and reproduced.

Both methods for computing mass balance are linear, so we estimate each of the corrections separately and combine them with the time series only at the last stage. The same holds for all of the trend corrections, especially the GIA correction which have been treated separately and added back in the last stage. This overall strategy allows us to analyze in details the relative weight of each of the components in our final results. The combination of data and corrections in the final result $M_F(t)$ is a simple sum:

$$M_F(t) = M_{\text{data}}(t) - M_{\text{GIA}}(t) + M_{\text{Deg-1}}(t) + M_{\text{GAC}}(t) \quad (1)$$

where the $M_x(t)$ is the mass changes time series and the subscript x indicates the source of each contribution: the uncorrected data (data), the GIA correction (GIA), the degree-1 correction (Deg-1) and the GAC correction (GAC).

For each basin, for each method and each data set we compute the mass balance (with its propagated uncertainties) for each available month. So for each basin we have four time series using GRACE data RL04 and four using the RL05 ones. We computed for each basin three time series for the degree-1 correction and two for the GAC correction (the difference GAC[04–05] and the fitted function). One of the degree-1 time series is provided on much denser timescale than monthly, so we perform an averaging procedure. The majority of the time series do not share the same exact

Variability of mass changes

V. R. Barletta et al.

Title Page

Abstract

Introduction

Conclusions

References

Tables

Figures

◀

▶

◀

▶

Back

Close

Full Screen / Esc

Printer-friendly Version

Interactive Discussion



sequence of months, so we select only the common months for each comparison and combination in order to maximize the number of available months in each case.

Once we have two or more time series to be compared and/or combined to produce a best estimate, the first way that comes to mind is to perform a simple average and to extract the standard deviation. However, different linear trends (and offsets) in time series act as a systematic bias. This spoils the statistical assumption which the standard deviation is based on, i.e. a gaussian distribution around the mean value. For this reason we separate the discussion of trend estimate from the monthly solutions.

Two time series $M_1(t)$ and $M_2(t)$ can differ for an overall factor m (regression index) and an overall offset q , and they can show also other kind of time dependent differences $\epsilon(t)$, e.g. $M_1(t) = mM_2(t) + q + \epsilon(t)$. We first identify the regression index and the offset with a least square fitting procedure and remove it in order to analyze just the monthly difference between the time series. When we analyse the difference for each basin between two time series, we compute

$$\delta_{12} = \sqrt{\sum_t \epsilon(t)^2} = \sqrt{\sum_t (M_1(t) - mM_2(t) - q)^2} \quad (2)$$

Assumption RI: by assuming that the regression index m mostly accounts for the difference in the trends rather than the $\epsilon(t)$ components, the difference in the trends can be estimated by $\delta_{T_{12}} = T_1(1 - (1/m))$, where T_1 is the trend of the series $M_1(t)$. When the above assumption on regression index m is not verified the $(\delta_{T_{12}}/T_1)$ shows in percent how much the regression index deviates from one. If the regression index m is close to one, the two time series do not need to be scaled relative to each other.

For averaging the time series we follow a similar strategy: we first find the average between N time series, $M_i(t)$ with $i = 1 \dots N$, as $M_A(t) = \sum_i M_i(t)/N$, then we find, for each of the series $M_i(t)$, the regression index with respect to the average $M_A(t)$, i.e. the m_i and the q_i parameters, so that $M_A(t) = m_i M_i(t) + q_i + \epsilon_i(t)$ for each i . Then by rescaling each solution with these parameters we find for each series the monthly residual standard deviation with respect to the average (assuming normally distributed

Variability of mass changes

V. R. Barletta et al.

Title Page	
Abstract	Introduction
Conclusions	References
Tables	Figures
◀	▶
◀	▶
Back	Close
Full Screen / Esc	
Printer-friendly Version	
Interactive Discussion	



Discussion Paper | Discussion Paper | Discussion Paper | Discussion Paper | Discussion Paper

values):

$$\delta_A(t) = \sqrt{\frac{1}{N-1} \sum_i (M_A(t) - m_i M_i(t) - q_i)^2} \quad (3)$$

where $\delta_A(t)$ is considered as the accuracy error when averaging between time series obtained with different methods and different datasets. The monthly precision error (the 95% confidence interval) is $1.96 \cdot \sigma_A(t)$ computed from the monthly square sum of the $\sigma_i(t)$ of the time series. So the total error on $M_A(t)$ is:

$$\text{err}_{M_A}(t) = 1.96 \sigma_A(t) + \delta_A(t) \quad (4)$$

Extending the definition 2 for $\delta_{T_{12}}$, we define the quantity δ_{T_A} (assuming normally distributed values) as:

$$\delta_{T_A} = T_A \sqrt{\frac{1}{N-1} \sum_i \left(1 - \frac{1}{m_i}\right)^2} \quad (5)$$

where T_A is the trend of the average. Under the above assumption (Assumption RI) we can use δ_{T_A} as an estimate for the trend accuracy. So when comparing the trends (see Sect. 4), under the above assumption (Assumption RI), the regression index m is used (with a bit of license) to assess and show the difference in trends for one time series with respect to another or with respect to the average.

The trend on the time series is computed with a weighted least square fitting procedure using a function composed by a linear trend, annual and semiannual term, and a constant. As for the monthly weight we use the monthly error of the time series. The precision error (the 95% confidence interval) $1.96 \cdot \sigma_{T_A}$ for the trend is computed using the variance of the fit.

Note about q : all our GRACE derived mass changes are computed with respect to the same reference gravity model, so they should have small or none q offset one from another. We find that small offset difference between data obtained with different release and methods exists.

4 Results and discussion

All the monthly time series shown in the following pictures are not corrected for the trend contribution of degree-1 and GIA, but these are accounted for when analyzing the trend.

5 We perform a cross validation of the two methods using both CSR and GFZ GRACE data. We compared all the 27 + 7 basin time series, and in addition to the discussion of the results for all of them, we show one example for each region, Antarctica and Greenland.

10 A general good agreement between the two methods for each of the data sets (CSR and GFZ) for each basin is clear by a simple visual inspection (pictures for each basins are in the Supplement). This agreement is particularly clear in the Amundsen sector (Fig. 4a, Antarctica-basin 21), and in South West Greenland (Fig. 4b, Greenland-basin 6), that we choose as example. By visual inspection the time series for the inversion (“i”, solid lines) and the conversion method (“c”, dash-dotted lines) overlap over almost the
15 entire time interval, for both data sets, CSR (blue) and GFZ (red) lines. For each basin, we quantify the agreement in the time series, regardless of the trend as explained in Sect. 3.5, by using the δ_{12} (Eq. 2), computed for each basin with respect to the average monthly error (Fig. 4c). We find that the differences between the two methods (light-purple bars) are much smaller than the differences (light-green bars) between the use
20 of CSR and GFZ, for almost all basins: the basins 19 and 25 show the same amount of difference between the two methods and the use of different datasets. The basin 25 is the smallest so either resolution or leakage can give noisy signal. Basin 19 has a very small trend and it is very close to basin 20 which has one of the strongest trend, so resolution or leakage can give again noisy signal.

25 The different combinations of methods and data sets also result in different trends in the mass time series. This difference is quantified by the linear relation, the regression index m and offset q parameters (as explained in Sect. 3.5), between two time series (shown in the small dispersion graph inside each of the two plots of Fig. 4a, b). The two

TCD

6, 3397–3446, 2012

Variability of mass changes

V. R. Barletta et al.

Title Page

Abstract

Introduction

Conclusions

References

Tables

Figures

◀

▶

◀

▶

Back

Close

Full Screen / Esc

Printer-friendly Version

Interactive Discussion



datasets (green dots) in the Amundsen sector produce a difference in regression index of 11 % and the two methods (purple squares) only 1 %. For Southwest Greenland the differences in regression index are closer, i.e. 6 % vs. 8 %.

We analyse the relative difference in regression index for each basin (Fig. 4c) caused by the two methods (purple bars) and the two datasets (green bars). We find that for almost all basins, the use of CSR data results in a larger trend than the GFZ (the green bars are almost all positive). For small basins (area, indicated in the vertical axes of Fig. 4c, smaller than 0.1 million km²) the two methods result in differences in regression index between 20 % and 30 %, larger than the error on the trends (the grey bars) and than the difference produced by the two datasets. For almost all the large basins, the two methods give smaller differences in regression index than the use of two datasets.

The differences between the use of RL04 and RL05 data are also related to the difference GAC[04–05] in their de-aliasing product (green line in Fig. 1) at basin scale. The sudden jump in 2009 is clearly visible in some of the basins, but it is not present in all. The fitted function $M_{\text{GAC}}(t)$ for each basin well reproduces the jump (orange line) and its standard deviation (grey band) account for the possible variability during the full GRACE period.

In order to compare the two distributions as discussed in Sect. 3.5, we correct our RL04 solution using the GAC[04–05] and we compare it with the RL05 just for the inversion method (Fig. 5). The results obtained from the two releases are quite different. The difference are in many basins larger for GFZ than for CSR (light-red bars larger than light-blue), especially for the large basins. Except for a few basins, the RL05 data produces smaller trends than the RL04. The lowest harmonics could be the most likely candidates but the true cause can be deeply buried in the new GRACE processing.

Yet another important contribution to the mass change variability comes from the degree-1 correction (see Sect. 2.3). The sensitivity kernel for degree-1 (Tables 1 and 2) can also be interpreted as the relative weight of each component X , Y and Z of the geocenter motion on each basin. From Table 1, it is clear that the basin 17 in Antarctica is the most affected by degree-1, but it is also the largest basin, and it is

Variability of mass changes

V. R. Barletta et al.

Title Page

Abstract

Introduction

Conclusions

References

Tables

Figures

◀

▶

◀

▶

Back

Close

Full Screen / Esc

Printer-friendly Version

Interactive Discussion



quite straightforward to see that the impact of the degree-1 is proportional to the area of the basin. The three degree-1 time series obtained with this sensitivity kernel (Table 1 and 2) and the three geocenter motion detrended time series have quite similar phase but different amplitude (two examples in Fig. 6).

The mass changes time series are the sum of four contributions (Eq. 1, Fig. 7). When estimating the errors on the monthly mass changes, we neglect the GIA because it only gives a contribution to the trend. For taking into account the effect of using different data sets, we use the monthly average (Sect. 3.5) and its error (Eq. 4), being both precision (blue band) and accuracy (light blue band) errors. We then add the monthly average of the degree-1 and its standard deviation (green band), and as a last step, we add the GAC correction $M_{\text{GAC}}(t)$ and its standard deviation (yellow band). We find that the degree-1 variability, represented by the monthly standard deviation with respect to the monthly average (green band), has a considerable impact on the total error as can be appreciated in Fig. 7c where it is presented as average per basin with respect to the average of the total error. The monthly variability of the GAC correction is quite small but not negligible (the yellow bars). The average of the accuracy error (light blue bars) represents the variability in the use of different method and different datasets and its impact on the total error is comparable with the degree-1 variability. The three sources of monthly variability together (the accuracy, the degree-1 and the GAC) are for almost all the basins larger than the precision error propagated from the data alone, i.e. the blue bars are almost all below the 50 %.

The basins 20, 21 and 22 (in front of the Amundsen Sea) have the largest trend in Antarctica (Fig. 8c). Amundsen sector (basin 21 and 22) has also the lowest relative errors (violet bars in Fig. 8a). In the Amundsen sector also all the other contributions different from the GRACE data (the blue bar, Fig. 8a) have a very small impact, namely the degree-1 (sky-blue bars, Fig. 8a), the GIA (green bars) and also the GAC (orange bars) corrections.

Due to its character, the GIA correction has been computed separately (Sect. 2.5). We compute the four GIA corrections described in Sect. 2.5 (Table 4), but we show its

Variability of mass changes

V. R. Barletta et al.

[Title Page](#)[Abstract](#)[Introduction](#)[Conclusions](#)[References](#)[Tables](#)[Figures](#)[◀](#)[▶](#)[◀](#)[▶](#)[Back](#)[Close](#)[Full Screen / Esc](#)[Printer-friendly Version](#)[Interactive Discussion](#)

Variability of mass changes

V. R. Barletta et al.

[Title Page](#)[Abstract](#)[Introduction](#)[Conclusions](#)[References](#)[Tables](#)[Figures](#)[I◀](#)[▶I](#)[◀](#)[▶](#)[Back](#)[Close](#)[Full Screen / Esc](#)[Printer-friendly Version](#)[Interactive Discussion](#)

relative contribution only for the average of the model Riva09 and IJ05-LV (green bars, Fig. 8a). Each of the four GIA corrections contribute to the trend with quite different proportions, and this becomes clear when observing the GIA variability (Max–Min) (green bars, Fig. 8b). So the average of all the corrections is not very meaningful nor representative, and in some cases, when the maximum and minimum value among the four GIA correction have opposite sign, the average is zero. The Riva09 and IJ05-LV in the typical GIA basin (1, 2, 18) give similar corrections, and in some large basin in East Antarctica (17, 2, 3, 10 for example) they both show much smaller correction than both the ICE5g (VM2-compressible and LV-low viscosity). Using the average of the model Riva09 and IJ05-LV is just one reasonable choice among other reasonable choices.

The GIA variability (Fig. 8b) is largest in most of the largest basins. However the most typical GIA pattern affects mainly basins 1, 2, 18 and 19, which are among those with largest GIA trend. In several basins, the GIA contribution (green bars, Fig. 8a) is significant compared to the data trend (blue bars) and in basin 17, 15, 2, 19, 11 and 24 it is dominant. So the GIA contribution has a relative importance also in basins not within the typical GIA regions, but which have small trends in the data (blue bar, Fig. 8c), e.g. as in basins 17, 15, 11 and 24.

The degree-1 contribution is not dominant in any of the basins (sky-blue bars, Fig. 8a), and it only exceeds 10% of the sum of contributions in those basins associated with a low mass trend (blue bar, Fig. 8c), e.g. in basins 17, 10, 11 and 16.

The GAC correction (orange bars, Fig. 8a) is more important than the degree-1 correction for almost all basin, and in some cases it has the same impact as the data trend (blue bars).

The accuracy errors on the trends (which account for difference between dataset and methods, and so also account for leakage errors) have about the same impact as the error on data trend computation (blue and light blue bars, Fig. 8d). It is interesting to notice that where the two largest data trend occur (blue bars, Fig. 8c), in basin 21 and 22 (Amundsen sector), we also find the largest (absolute) accuracy errors. However

basin 20, the third largest data trend, has one of the smallest accuracy error. As noticed above, the relative error for these basins are the smallest.

The degree-1 uncertainties on the trend, which are primarily caused by the GIA degree one uncertainties (sky-blue bars, Fig. 8d), are comparable with the GIA uncertainties (green bars) for many basin. And for both these contributions, the uncertainties are larger for larger basins.

The uncertainties on trend computation for the GAC correction are very small for all the basins (orange bars, Fig. 8d)

For Greenland the trends computed only on data are much more important than the correction contributions (Fig. 9a) and the errors are below 20 % for all basin but one, the largest. The largest basin (the number 2), in North-West Greenland has a small trend and small GIA correction which have similar contribution in the total trend. Also the GAC correction has the largest value in North-West Greenland.

The largest GIA variability is located in basin 6, South-West Greenland (green bars Fig. 9b) where also the largest total trend (blue bars, Fig. 9c) is found, and yet the trend on data in basin 6 dominate with almost 85 % of the total trend.

The degree-1 has small impact on the total trend (sky-blue bars, Fig. 9a) but they contribute to increase the total error on trend (sky-blue bars, Fig. 9d).

As the last result, we present the trends on four different periods (Table. 6) for our derived time series using the same configuration as in Figs. 8 and 9. The total mass balance for the whole GRACE period is found to be -234 Gtyr^{-1} for Greenland and -83 Gtyr^{-1} for Antarctica where most of the mass loss is going on in West Antarctica with -111 Gtyr^{-1} (errors are in Table 6). A more rapid mass loss clearly takes place in Greenland and West Antarctica (Table 6) in the second period of GRACE mission (August 2007–November 2011) compared to the first one (August 2002–July 2007).

This increase or acceleration is even clearer at basin scale (Figs. 10 and 11). For Antarctica, however, the acceleration in mass loss in most of the basins in the western part (Fig. 10) is counteracted by an increase of accumulation in the eastern part.

Variability of mass changes

V. R. Barletta et al.

Title Page

Abstract

Introduction

Conclusions

References

Tables

Figures

◀

▶

◀

▶

Back

Close

Full Screen / Esc

Printer-friendly Version

Interactive Discussion



In Western Greenland (Fig. 11) the mass loss increased in the last 5 yr, while in the eastern part the mass loss has decreased.

5 Conclusions

In the light of the consistent and systematic error analysis that we have performed, the results presented in this study are statistically meaningful.

For the first time the various sources of variability in mass change estimates have been systematically assessed, and we quantify their associated uncertainties for the mass trends as well as the monthly mass change solutions. We find an interesting difference between the results obtained with use of RL05 with respect to the use of RL04. This difference is within the error but the RL05 results in smaller trend in the majority of the basins. We suspect that this is due mostly to differences in the low degrees, however more targeted studies should be carried out to clarify this issue.

We cross validate our two independent methods, and the clear agreement between the two confirms that the low resolution of the input GRACE data allows us to use very simple leakage treatment like the one employed in the conversion method. A surprisingly large part of the variability in the monthly solution arises from the use of different data sets rather than different methods. However, the uncertainties on degree-1 also largely contribute to the variability in the monthly solutions.

The degree-1 is still an open issue, hence we build a degree-1 sensitivity kernel (at basin scale) which represents a solid and lasting tool to perform straightforward computation of the degree-1 correction on mass balance using any geocenter motion time series. For our preferred estimate, we then choose to use an average of three available geocenter motion time series based on different methods.

We show the impact of the correction for the de-aliasing GRACE product (GAC), especially on the trends in Antarctica mass balance, and we generate an alternative correction that can be applied to the whole RL04 time series, while we wait for the RL05 to be completely released and tested.

Variability of mass changes

V. R. Barletta et al.

Title Page

Abstract

Introduction

Conclusions

References

Tables

Figures

◀

▶

◀

▶

Back

Close

Full Screen / Esc

Printer-friendly Version

Interactive Discussion



The outcome of this systematic analysis is a set of our preferred monthly solutions and their associated error estimate which is a combination of precision error (propagated from the data) and accuracy error due to the method and the different data set. Furthermore, we provide our preferred degree-1, GIA and GAC corrections for both the monthly solution and the trends.

Since trends often depends on choice of the time interval, we compute trends over the whole period 2003–2011 and sub periods 2003–2006 and 2007–2011. We find a clear increase in ice loss in the sub-interval 2007–2011 only for West Antarctica and Greenland.

Supplementary material related to this article is available online at:
<http://www.the-cryosphere-discuss.net/6/3397/2012/tcd-6-3397-2012-supplement.pdf>.

Acknowledgements. This work was supported by funding to the ice2sea program from the European Union 7th Framework Program, grant number 226375 (ice2sea contribution number ice2sea116).

References

- Ackert Jr., R. P., Mukhopadhyay, S., Pollard, D., DeConto, R. M., Putnam, A. E., and Borns Jr., H. W.: West Antarctic Ice Sheet elevation in the Ohio Range: geologic constraints and ice sheet modelling prior to the last highstand, *Earth Planet. Sci. Lett.*, 307, 83–93, 2011.
- Bettadpur, S.: UTCSR level-2 processing standards document for level-2 product release 0004. GRACE 327–742, Center for Space Research, Univ. Texas, Austin, Technical report CSR-GR-03–03, available at: ftp://podaac.jpl.nasa.gov/allData/grace/docs/L2-CSR0004_ProcStd_v3.1.pdf, 17 pp., 2007. 3402
- Bettadpur, S. and the CSR Level-2 Team: Insights into the Earth System mass variability from CSR-RL05 GRACE gravity fields, *Geophysical Research Abstracts*, vol. 14, EGU2012-6409,

Variability of mass changes

V. R. Barletta et al.

Title Page

Abstract

Introduction

Conclusions

References

Tables

Figures

◀

▶

◀

▶

Back

Close

Full Screen / Esc

Printer-friendly Version

Interactive Discussion



Variability of mass changes

V. R. Barletta et al.

Title Page

Abstract

Introduction

Conclusions

References

Tables

Figures

◀

▶

◀

▶

Back

Close

Full Screen / Esc

Printer-friendly Version

Interactive Discussion



EGU General Assembly 2012, available at: http://www.csr.utexas.edu/grace/Bettadpur_RL05.pdf, 2012. 3402, 3403

Barletta, V. R., Bordoni, A., and Sabadini, R.: Isolating the PGR signal in the GRACE data: impact on mass balance estimates in Antarctica and Greenland, *Geophys. J. Int.*, 172, 18–30, doi:10.1111/j.1365-246X.2007.03630.x, 2008. 3399, 3407, 3412

Barletta, V. R. and Bordoni, A.: Clearing observed PGR in GRACE data aimed at global viscosity inversion: weighted mass trends technique, *Geophys. Res. Lett.*, 36, L02305, doi:10.1029/2008GL036429, 2009. 3407

Barletta, V. R. and Spada, G.: Assessment of errors and uncertainty patterns in GIA modeling, American Geophysical Union, Fall Meeting 2011, abstract #G21A-0796, 2011. 3408, 3409

Barletta, V. R., Bordoni, A., Aoudia, A., and Sabadini, R.: Squeezing more information out of time variable gravity data with a temporal decomposition approach, *Global Planet. Change*, 82/83, 51–64, doi:10.1016/j.gloplacha.2011.11.010, 2012a. 3400

Barletta, V. R., Spada, G.: Assessment of errors and uncertainty patterns in GIA modeling, EGU General Assembly 2012, *Geophysical Research Abstracts*, vol. 14, EGU2012-9717, available at: <http://meetingorganizer.copernicus.org/EGU2012/EGU2012-9717.pdf>, 2012b. 3408, 3409

Chambers, D. P.: Observing seasonal steric sea level variations with GRACE and satellite altimetry, *J. Geophys. Res.*, 111, C03010, doi:10.1029/2005JC002914, 2006. 3399, 3404

Chen, J. L., Wilson, C. R., and Tapley, B. D.: Satellite gravity measurements confirm accelerated melting of Greenland ice sheet, *Science*, 313, 1958–1960, doi:10.1126/science.1129007, 2006a. 3407

Chen, J. L., Wilson, C. R., Blankenship, D. D., and Tapley, B. D.: Antarctic mass rates from GRACE, *Geophys. Res. Lett.*, 33, L11502, doi:10.1029/2006GL026369, 2006b. 3399

Cheng, M. and Tapley, B. D.: Variations in the Earth's oblateness during the past 28 years, *J. Geophys. Res.*, 109, B09402, doi:10.1029/2004JB003028, 2004. 3402

Cheng, M., Ries, J., Tapley, B.: Geocenter variations from analysis of SLR data, IAG Commission 1 Symposium 2010, Reference Frames for Applications in Geosciences (REFAG2010), Marne-La-Vallée, France, 4–8 October, 2010. 3404, 3405, 3441

Dahle, C., Flechtner, F., Gruber, C., König, D., König, R., Michalak, G., and Neumayer, K. H.: GFZ GRACE Level-2 Processing Standards Document for Level-2 Product Release 0005, Scientific Technical Report – Data, 12/02, GeoForschungsZentrum Potsdam, Potsdam, Germany, 20 pp., doi:10.2312/GFZ.b103-12020, 2012a. 3402

Variability of mass changes

V. R. Barletta et al.

Title Page

Abstract

Introduction

Conclusions

References

Tables

Figures

◀

▶

◀

▶

Back

Close

Full Screen / Esc

Printer-friendly Version

Interactive Discussion



- Dahle, C., Flechtner, F., Gruber, C., König, D., König, R., Michalak, G., Neumayer, K. H.: The New GFZ RL05 GRACE Gravity Field Model Time Series, *Geophysical Research Abstracts*, vol. 14, EGU2012-10475, 2012, EGU General Assembly 2012, available at: http://presentations.copernicus.org/EGU2012-10475_presentation.pdf, 2012b. 3402
- 5 Farrel, W. E.: Deformation of the Earth by surface loads, *Rev. Geophys. Space Phys.*, 10, 762–795, 1972. 3410
- Flechtner, F.: GFZ Level-2 processing standards document for level-2 product release 0004, GeoForschungsZentrum Potsdam, Potsdam, Germany, 17 pp., 2007a. 3402
- Flechtner, F.: AOD1B Product description document for product releases 01 to 04, Geo-
- 10 ForschungsZentrum Potsdam, Potsdam, Germany, 17 pp., 2007b. 3403
- Fleming K., and Lambeck, K.: Constraints on the Greenland Ice Sheet since the Last Glacial Maximum from sea-level observations and glacial-rebound models, *Quaternary Sci. Rev.*, 23, 1053–1077, doi:10.1016/j.quascirev.2003.11.001, 2004. 3408
- Forsberg, R. and Reeh, N.: Mass change of the Greenland Ice Sheet from GRAC E, in: *Proceedings, Gravity Field of the Earth – 1st meeting of the International Gravity Field Service*, Harita Dergisi, Ankara, vol. 73, issue 18 (revised version), 2007. 3399, 3410
- 15 Gunter, B., Riva, R., Urban, T., Schutz, B., Harpold, R., Helsen, M., and Nagel, P.: Evaluation of GRACE and ICESat mass change estimates over Antarctica, in: *Proceedings of the IAG International Symposium on Gravity, Geoid and Earth Observation (GGEO)*, Chania, Greece, 2008. 3407
- 20 Gunter, B., Urban, T., Riva, R., Helsen, M., Harpold, R., Poole, S., Nagel, P., Schutz, B., Tapley, B. : A comparison of coincident GRACE and ICESat data over Antarctica, *J. Geodesy*, 83, 1051–1060, doi:10.1007/s00190-009-0323-4, 2009. 3407
- Hardy, R., Bamber, J., and Orford, S.: The delineation of drainage basins on the Greenland ice sheet for mass-balance analyses using a combined modelling and geographical information system approach, *Hydrol. Process.*, 14, 1931–1941, 2000. 3412
- 25 Horwath, M. and Dietrich, R.: Signal and error in mass change inferences from GRACE: the case of Antarctica, *Geophys. J. Int.*, 177, 849–864 doi:10.1111/j.1365-246X.2009.04139.x, 2009. 3400, 3407, 3410, 3412
- 30 IPCC 2007, Solomon, S.: *Climate Change 2007: The Physical Science Basis: Contribution of Working Group I to the Fourth Assessment Report of the Intergovernmental Panel on Climate Change*, Cambridge Univ. Press, 2007. 3398

- Ivins, E. R. and James, T. S.: Antarctic glacial isostatic adjustment: a new assessment, *Antarct. Sci.*, 17, 541–553, doi:10.1017/S0954102005002968, 2005. 3406
- Klemann, V. and Martinec, Z.: Contribution of glacial-isostatic adjustment to the geocenter motion, *Tectonophysics*, 511, 99–108, doi:10.1016/j.tecto.2009.08.031, 2011 (2009 online first). 3404, 3405, 3432
- 5 Kusche, J., Schmidt, R., Petrovic, S., and Rietbroek, R.: Decorrelated GRACE Time-Variable Gravity Solutions by GFZ, and their Validation using a Hydrological Model, *J. Geodesy*, 83, 903–913, doi:10.1007/s00190-009-0308-3, 2009. 3406
- Luthcke, S. B., Zwally, H. J., Abdalati, W., Rowlands, D. D., Ray, R. D., Nerem, R. S., Lemoine, F. G., McCarthy, J. J., and Chinn, D. S.: Recent Greenland ice mass loss by drainage system from satellite gravity observations, *Science*, 314, 1286–1289, 2006. 3399, 3400
- 10 Mackintosh, A., Golledge, N., Domack, E., Dunbar, R., Leventer, A., White, D., Pollard, D., DeConto, R., Fink, D., Zwartz, D., Gore, D., and Lavoie, C.: Retreat of the East Antarctic ice sheet during the last glacial termination, *Nat. Geosci.*, 4, 195–202, 2011. 3407
- Mitrovica, J. X. and Peltier, W. R.: On postglacial geoid subsidence over the equatorial oceans, *J. Geophys. Res.*, 96, 20053–20071, 1991.
- Mitrovica, J. X., Wahr, J., Matsuyama, I., and Paulson, A.: The rotational stability of an Ice Age Earth, *Geophys. J. Int.*, 161, 491–506, 2005. 3406
- 20 Paulson, A., Zhong, S., and Wahr, J.: Inference of mantle viscosity from GRACE and relative sea level data, *Geophys. J. Int.*, 171, 497–508, doi:10.1111/j.1365-246X.2007.03556.x, 2007. 3406, 3408
- Peltier, W. R.: Global Glacial Isostasy and the Surface of the Ice-Age Earth: the ICE-5G(VM2) model and GRACE, *Ann. Rev. Earth Planet. Sci.*, 32, 111–149, 2004. 3406, 3407
- 25 Ramillien, G., Lombart, A., Cazenave, A., Ivins, E. R., Llubes, M., Remy, F., Biancale, R.: Interannual variations of the mass balance of the Antarctica and Greenland ice sheets from GRACE, *Global Planet. Change*, 53, 198–208, doi:10.1016/j.gloplacha.2006.06.003, 2006. 3399
- Rietbroek, R., Fritsche, M., Brunnabend, S.-E., Daras, I., Kusche, J., Schroter, J., Flechtner, F., and Dietrich, R.: Global surface mass from a new combination of GRACE, modelled OBP and reprocessed GPS data, *J. Geodyn.*, 59–60, 64–71, doi:10.1016/j.jog.2011.02.003, 2012a. 3404, 3405, 3441
- 30

Variability of mass changes

V. R. Barletta et al.

Title Page

Abstract

Introduction

Conclusions

References

Tables

Figures

I◀

▶I

◀

▶

Back

Close

Full Screen / Esc

Printer-friendly Version

Interactive Discussion



Variability of mass changes

V. R. Barletta et al.

Title Page

Abstract

Introduction

Conclusions

References

Tables

Figures

◀

▶

◀

▶

Back

Close

Full Screen / Esc

Printer-friendly Version

Interactive Discussion



- Rietbroek, R., Brunnabend, S.-E., Schröter, J., Kusche, J.: Resolving ice sheet mass balance by fitting fingerprints to GRACE and altimetry, *J. Geodyn.*, 59–60, 72–81, doi:10.1016/j.jog.2011.06.007, 2012b. 3405, 3432
- 5 Riva, R. E. M., Gunter, B. C., Urban, T. J., Vermeersen, B. L. A., Lindenbergh, R. C., Helsen, M. M., Bamber, J. L., van de Wal, R. S. W., van den Broeke, M. R., and Schutz, B. E.: Glacial isostatic adjustment over Antarctica from combined ICESat and GRACE satellite data, *Earth Planet. Sci. Lett.*, 288, 516–523, doi:10.1016/j.epsl.2009.10.013 2009. 3407, 3408
- 10 Riva, R. E. M., van der Wal, W., Lavallée, D. A., Hashemi Farahani, H., and Ditmar, P.: Geocenter motion due to surface mass transport from GRACE satellite data, *Geophys. Res. Abstr.*, vol. 14, EGU2012-9620, 2012 EGU General Assembly 2012, available at: <http://meetingorganizer.copernicus.org/EGU2012/EGU2012-9620.pdf>, 2012. 3404
- 15 Sasgen, I., Broeke, M. v. d., Bamber, J. L., Rignot, E., Sandberg Sørensen, L., Wouters, B., Martinec, Z., Velicogna, I., and Simonsen, S. B.: Timing and origin of recent regional ice-mass loss in Greenland, *Earth Planet. Sci. Lett.*, 333–334, 293–303, doi:10.1016/j.epsl.2012.03.033, 2012. 3399
- Schrama, E. J. O. and Wouters, B.: Revisiting Greenland ice sheet mass loss observed by GRACE, *J. Geophys. Res.*, 116, B02407, doi:10.1029/2009JB006847, 2011. 3399, 3400
- 20 Spada, G., Antonioli, A., Boschi, L., Cianetti, S., Galvani, G., Giunchi, C., Perniola, B., Piana Agostinetti, N., Piersanti, A., and Stocchi, P.: Modeling Earth's post-glacial rebound, *EOS*, 85, 62–64, 2004. 3408
- Spada, G., Barletta, V. R., Klemann, V., Riva, R. E. M., Martinec, Z., Gasperini, P., Lund, B., Wolf, D., Vermeersen, L. L. A., and King, M. A.: A benchmark study for glacial isostatic adjustment codes, *Geophys. J. Int.*, 185, 106–132, doi:10.1111/j.1365-246X.2011.04952.x, 2011. 3408
- 25 Spada, G., Barletta, V. R., Klemann, V., van der Wal, W., James, T. S., Simon, K., Riva, R. E. M., Martinec, Z., Gasperini, P., Lund, B., Wolf, D., Vermeersen, L. L. A., and King, M. A.: Benchmarking and testing the “Sea Level Equation”: the COST ES0701 experience, *Geophysical Research Abstracts*, vol. 14, EGU2012-9773, EGU General Assembly, 2012. 3408
- 30 Steffen, H., Wu, P., and Wang, H.: Determination of the Earth's structure in Fennoscandia from GRACE and implications for the optimal post-processing of GRACE data, *Geophys. J. Int.*, 182, 1295–1310, doi:10.1111/j.1365-246X.2010.04718.x, 2010. 3400

Swenson, S. and Wahr, J.: Methods for inferring regional surfacemass anomalies from GRACE measurements of time-variable gravity, *J. Geophys. Res.*, 107, 2193, doi:10.1029/2001JB000576, 2002.

Swenson, S. and Wahr, J.: Post-processing removal of correlated errors in GRACE data, *Geophys. Res. Lett.*, 33, L08402, doi:10.1029/2005GL025285, 2006. 3405

Swenson, S., Chambers, D., and Wahr, J.: Estimating geocenter variations from a combination of GRACE and ocean model output, *J. Geophys. Res.*, 113, B08410, 2008. 3404, 3405, 3432, 3441

Sørensen, L. S. and Forsberg, R.: Greenland ice sheet mass loss from GRACE monthly models, gravity, *Geoid Earth Obs.*, 135, 527–532, doi:10.1007/978-3-642-10634-7_70, 2010. 3400, 3410

Sørensen, L. S., Simonsen, S. B., Nielsen, K., Lucas-Picher, P., Spada, G., Adalgeirsdottir, G., Forsberg, R., and Hvidberg, C. S.: Mass balance of the Greenland ice sheet (2003–2008) from ICESat data – the impact of interpolation, sampling and firn density, *The Cryosphere*, 5, 173–186, doi:10.5194/tc-5-173-2011, 2011.

Tegmark, M.: An icosahedron-based method for pixelizing the celestial sphere, *Astrophys. J. Lett.*, 470, L81–L84, 1996. 3411, 3437

Thomas, I. D., King, M. A., Bentley, M. J., Whitehouse, P. L., Penna, N. T., Williams, S. D. P., Riva, R. E. M., Lavallee, D. A., Clarke, P. J., King, E. C., Hindmarsh, R. C. A., and Koivula, H.: Widespread low rates of Antarctic glacial isostatic adjustment revealed by GPS observations, *Geophys. Res. Lett.*, 38, L22302, doi:10.1029/2011GL049277, 2011. 3407

Todd, C., Stone, J., Conway, H., Hall, B., and Bromley, G.: Late Quaternary evolution of Reedy Glacier, Antarctica, *Quaternary Sci. Rev.*, 29, 1328–1341, 2010. 3407

Tscherning, C. C., Arabelos, D., and Strykowski, G.: The 1-cm geoid after GOC E, *The IAG Symposia*, 123, 267–270, 2001. 3413

Velicogna, I. and Wahr, J.: Greenland mass balance from GRACE, *Geophys. Res. Lett.*, 32, L18505, doi:10.1029/2005GL023955, 2005. 3399, 3400, 3412

Velicogna, I. and Wahr, J.: Measurements of time-variable gravity show mass loss in Antarctica, *Science*, 311, 1754–1756, doi:10.1126/science.1123785, 2006. 3399

Velicogna, I.: Increasing rates of ice mass loss from the Greenland and Antarctic ice sheets revealed by GRACE, *Geophys. Res. Lett.*, 36, L19503, doi:10.1029/2009GL040222, 2009. 3399

TCO

6, 3397–3446, 2012

Variability of mass changes

V. R. Barletta et al.

Title Page

Abstract

Introduction

Conclusions

References

Tables

Figures

◀

▶

◀

▶

Back

Close

Full Screen / Esc

Printer-friendly Version

Interactive Discussion



Variability of mass changes

V. R. Barletta et al.

Title Page

Abstract

Introduction

Conclusions

References

Tables

Figures

I◀

▶I

◀

▶

Back

Close

Full Screen / Esc

Printer-friendly Version

Interactive Discussion



- Wahr, J., Molenaar, M., and Bryan F.: Time-variability of the Earth's gravity field: hydrological and oceanic effects and their possible detection using GRACE, *J. Geophys. Res.*, 103, 20530, doi:10.1029/98JB02844, 1998. 3410, 3412
- 5 Wouters, B., Chambers, D., and Schrama, E. J. O.: GRACE observes small-scale mass loss in Greenland, *Geophys. Res. Lett.*, 35, L20501, doi:10.1029/2008GL034816, 2008. 3399
- Wu, X., Heflin, M. B., Schotman, H., Vermeersen, L. L. A., Dong, D., Gross, R. S., Ivins, E. R., Moore, A. W., and Owen, S. E.: Simultaneous estimation of global present-day water transport and glacial isostatic adjustment, *Nat. Geosci.*, 3, 642–646, doi:10.1038/ngeo938, 2010. 3407
- 10 Wu, X., Ray, J., and van Dam, T.: Geocenter motion and its geodetic and geophysical implications, *J. Geodyn.*, 58, 44–61, doi:10.1016/j.jog.2012.01.007, 2012. 3400, 3404, 3405, 3432
- Zwally, H. J., Giovinetto, M. B., Beckley, M. A., and Saba, J. L.: Antarctic and Greenland Drainage Systems, GSFC Cryospheric Sciences Laboratory, available at: http://icesat4.gsfc.nasa.gov/cryo_data/ant_grn_drainage_systems.php, 2012. 3413

Variability of mass changes

V. R. Barletta et al.

Title Page

Abstract

Introduction

Conclusions

References

Tables

Figures

◀

▶

◀

▶

Back

Close

Full Screen / Esc

Printer-friendly Version

Interactive Discussion



Table 1. Degree1 sensitivity kernel for Antarctica. The first column indicate the basin number (or region), the second its area, the other three columns indicate the variation in Gt due to 1 mm of variation in the geocenter coordinates X , Y and Z (in Gtmm^{-1}). Two spherical caps of the dimension of the Polar Gaps (PG) and three macro regions, Antarctic Peninsula (AP), West (WA) and East Antarctica (EA), are also computed.

B.n.	Area	X	Y	Z
25-AP	0.03	0.18	-0.39	-0.97
27-AP	0.04	0.18	-0.26	-1.03
26-AP	0.04	0.39	-0.70	-1.73
23-WA	0.06	-0.04	-0.48	-1.47
15-EA	0.10	-0.66	0.15	-1.90
24-AP	0.11	0.17	-0.58	-1.73
9-EA	0.12	0.17	0.39	-1.17
8-EA	0.13	0.37	0.65	-1.75
5-EA	0.14	0.49	-0.02	-1.49
20-WA	0.15	-0.58	-0.53	-2.92
22-WA	0.17	-0.05	-0.33	-1.26
21-WA	0.18	-0.16	-0.38	-1.70
18-WA	0.20	-0.22	-0.20	-2.21
4-EA	0.20	0.79	-0.29	-3.02
16-EA	0.22	-0.45	0.20	-1.93
11-EA	0.23	0.09	0.46	-1.57
19-WA	0.26	-0.33	-0.22	-2.33
1-WA	0.35	0.26	-0.77	-4.30
7-EA	0.37	0.95	0.94	-3.61
6-EA	0.47	1.42	0.54	-4.58
14-EA	0.55	-1.52	1.12	-4.96
2-EA	0.56	0.17	-0.13	-4.78
12-EA	0.59	-0.05	2.16	-5.48
10-EA	0.70	0.46	0.99	-4.77
13-EA	0.87	-1.13	2.25	-6.94
3-EA	1.20	1.34	0.17	-8.88
17-EA	1.36	-1.02	0.98	-11.10
PG (-81.5)		-0.02	-0.11	-16.05
PG (-86.0)		0.03	-0.01	-3.30
AP	0.22	0.92	-1.93	-5.47
WA	1.37	-1.11	-2.92	-16.19
EA	7.79	1.44	10.58	-67.93
AIS	9.38	1.24	5.73	-89.59

Variability of mass changes

V. R. Barletta et al.

Table 2. Degree1 sensitivity kernel for Greenland. The first column indicate the basin number (or region), the second its area, the other 3 columns indicate the variation in Gt due to 1 mm of variation in the geocenter coordinates X , Y and Z (Gtmm^{-1}).

B.n.	Area	X	Y	Z
5	0.05	0.62	-0.63	1.64
4	0.11	0.60	-0.42	1.49
1	0.17	0.21	-0.20	2.12
3	0.20	1.14	-0.58	3.43
7	0.21	0.47	-0.72	3.10
6	0.32	1.02	-1.37	4.18
2	0.36	0.98	-0.41	4.97
GRIS	1.42	20.93	-4.31	5.04

Title Page

Abstract

Introduction

Conclusions

References

Tables

Figures

I◀

▶I

◀

▶

Back

Close

Full Screen / Esc

Printer-friendly Version

Interactive Discussion



Variability of mass changes

V. R. Barletta et al.

Table 4. GIA trends for Antarctica. The first column is the basin number, the second its area (in 10^6 km^2) and from the third column the values are in Gt yr^{-1} , and they report the values for the four models, namely ICE5g-VM2 compressible with rotational feedback, Riva09, IJ05-LV and ICE5g-LV. The last column reports the maximum uncertainty among the last three models. The basins are sorted from the smallest to the largest.

N.	Area	i5g-CP	Riva09	IJ05-LV	I5G-LV	Unc.
25	0.03	1.50	0.10	0.58	0.36	0.08
27	0.04	2.21	1.48	1.78	1.01	0.21
26	0.04	2.22	-0.51	0.67	0.50	0.11
23	0.06	0.78	2.04	1.79	0.87	0.26
15	0.10	0.26	-0.25	-0.03	0.39	0.22
24	0.11	4.84	4.61	4.06	1.61	0.46
9	0.12	1.42	2.31	1.09	0.65	0.23
8	0.13	2.17	3.18	0.59	0.71	0.12
5	0.14	0.16	2.03	0.22	0.18	0.18
20	0.15	1.50	-1.47	2.11	2.10	0.56
22	0.17	1.67	2.19	2.95	1.43	0.28
21	0.18	3.07	3.02	1.81	1.95	0.41
18	0.20	13.53	4.90	4.82	4.79	0.63
4	0.20	1.71	4.19	1.87	1.34	0.51
16	0.22	1.55	0.46	0.07	1.39	0.31
11	0.23	1.45	0.83	1.11	1.04	0.20
19	0.26	13.09	2.88	5.24	4.79	0.63
1	0.35	18.83	13.89	13.30	8.28	1.30
7	0.37	2.27	3.14	0.39	1.21	0.25
6	0.47	1.08	5.14	0.51	0.96	0.48
14	0.55	0.61	0.23	1.84	1.12	0.52
2	0.56	16.14	4.48	4.25	8.90	1.11
12	0.59	3.06	4.24	1.53	2.50	0.33
10	0.70	5.85	-0.13	0.53	3.67	0.72
13	0.87	4.54	6.25	1.07	3.08	0.57
3	1.20	13.32	2.61	4.36	9.30	1.77
17	1.36	21.83	7.74	4.22	14.65	2.25
EA	7.79	77.41	46.44	23.61	51.10	8.92
WA	1.37	52.47	27.44	32.03	24.20	2.72
AP	0.22	10.77	5.68	7.09	3.47	0.78
AIS	9.38	140.65	79.56	62.72	78.77	11.23

[Title Page](#)
[Abstract](#)
[Introduction](#)
[Conclusions](#)
[References](#)
[Tables](#)
[Figures](#)
[I◀](#)
[▶I](#)
[◀](#)
[▶](#)
[Back](#)
[Close](#)
[Full Screen / Esc](#)
[Printer-friendly Version](#)
[Interactive Discussion](#)


Variability of mass changes

V. R. Barletta et al.

Table 5. GIA trends for Greenland. The first column is the basin number, the second its area (in 10^6 km^2) and from the third column the values are in Gt yr^{-1} , and they report the values for the three models, namely ICE5g-VM2 compressible with rotational feedback, ANU, ICE5g-VM2 incompressible without rotation. The last column reports the maximum uncertainty among the models. The basins are sorted from the smallest to the largest.

N.	Area	i5g-CP	ANU	i5g	Unc.
5	0.05	-1.32	-0.40	-1.11	0.71
4	0.11	-1.21	0.22	-0.43	0.58
1	0.17	3.15	3.41	3.77	0.84
3	0.20	-0.95	1.56	0.11	1.03
7	0.21	-1.87	0.09	-2.09	1.73
6	0.32	-6.82	2.37	-3.47	3.80
2	0.36	3.73	2.21	4.61	1.16
GRIS	1.42	-5.29	9.47	1.40	7.17

Title Page

Abstract

Introduction

Conclusions

References

Tables

Figures

◀

▶

◀

▶

Back

Close

Full Screen / Esc

Printer-friendly Version

Interactive Discussion



Variability of mass changes

V. R. Barletta et al.

Table 6. Trends (in Gt yr^{-1}) for Greenland Ice Sheets (GRIS) and for Antarctica Ice Sheets (AIS) three macro regions: Antarctic Peninsula (AP), West (WA) and East Antarctica (EA).

Region	Jan 2003–Nov 2011	Oct 2003–Nov 2008	Aug 2002–Jul 2007	Aug 2007–Nov 2011
AP	-24.04 ± 5.42	-16.48 ± 7.72	-5.34 ± 7.87	-33.94 ± 8.19
WA	-110.60 ± 14.66	-65.48 ± 16.38	-50.28 ± 16.85	-195.00 ± 18.89
EA	51.97 ± 29.07	21.95 ± 33.53	52.49 ± 34.11	108.37 ± 38.59
AIS	-82.67 ± 37.50	-60.01 ± 43.30	-3.14 ± 43.97	-120.58 ± 51.03
GRIS	-234.01 ± 20.49	-210.63 ± 22.80	-178.74 ± 22.44	-275.97 ± 27.27

Title Page

Abstract

Introduction

Conclusions

References

Tables

Figures

I◀

▶I

◀

▶

Back

Close

Full Screen / Esc

Printer-friendly Version

Interactive Discussion



Variability of mass changes

V. R. Barletta et al.

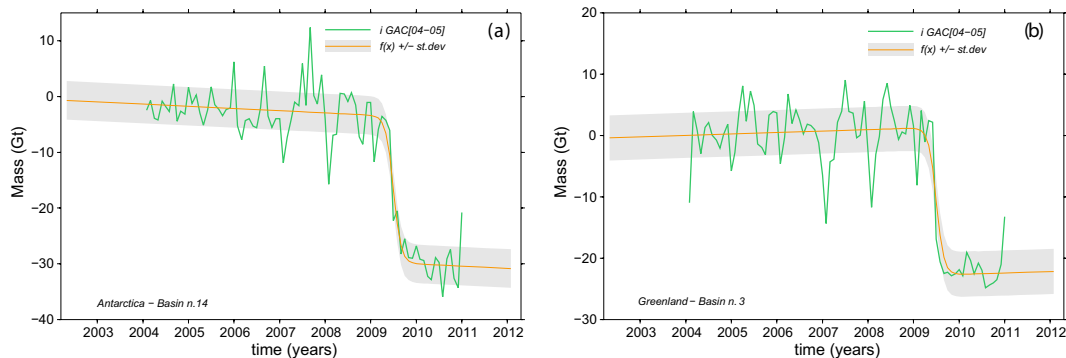


Fig. 1. Difference between the GAC-RL04 and the GAC-RL05 (green line), and the fitted function (orange line) with its standard deviation (grey band). Solution for basin 14 for Antarctica **(a)** and basin 3 for Greenland **(b)**.

Title Page

Abstract

Introduction

Conclusions

References

Tables

Figures

◀

▶

◀

▶

Back

Close

Full Screen / Esc

Printer-friendly Version

Interactive Discussion



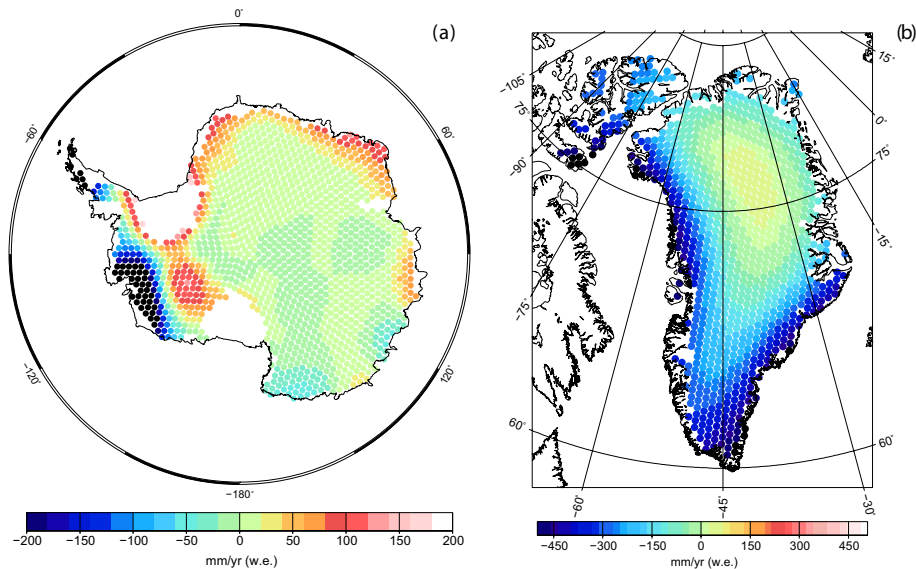


Fig. 2. Point mass solution for the trend in Antarctica **(a)** and Greenland **(b)** for the inversion method (Method 1). The mass points are inverted on an icosahedron-based grids (Tegmark, 1996), using disks of about 40 and 20 km radius for Antarctica and Greenland.

Variability of mass changes

V. R. Barletta et al.

Title Page

Abstract

Introduction

Conclusions

References

Tables

Figures

◀

▶

◀

▶

Back

Close

Full Screen / Esc

Printer-friendly Version

Interactive Discussion



Variability of mass changes

V. R. Barletta et al.

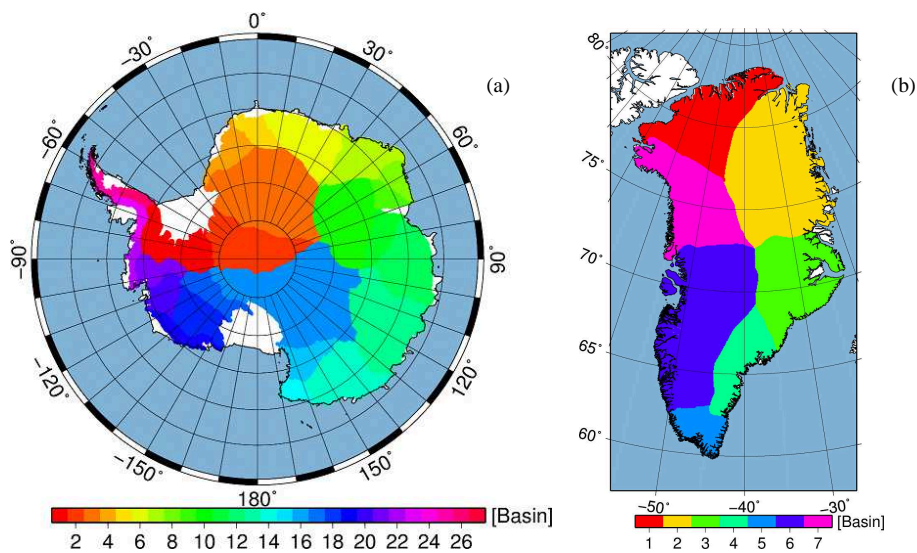


Fig. 3. Basins definitions for Antarctica **(a)** and Greenland **(b)** used in this work.

Title Page

Abstract

Introduction

Conclusions

References

Tables

Figures

I◀

▶I

◀

▶

Back

Close

Full Screen / Esc

Printer-friendly Version

Interactive Discussion



Variability of mass changes

V. R. Barletta et al.

Title Page

Abstract

Introduction

Conclusions

References

Tables

Figures

◀

▶

◀

▶

Back

Close

Full Screen / Esc

Printer-friendly Version

Interactive Discussion

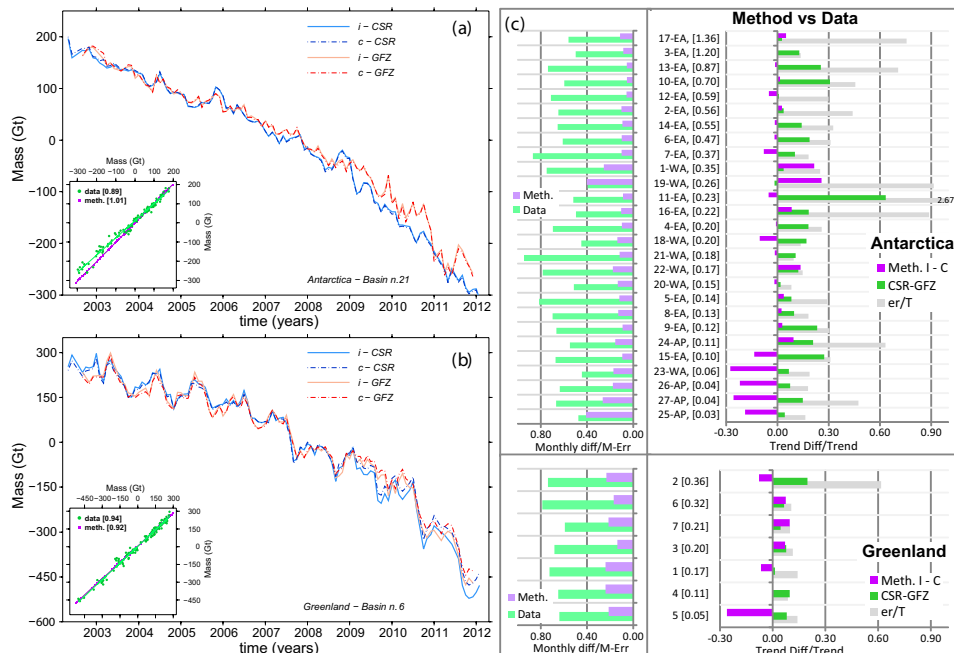


Fig. 4. RL04 monthly solution for basin 21 for Antarctica **(a)** in Amundsen sector and basin 6 for Greenland **(b)**. Comparison between the two methods and two data sets (CSR and GFZ): in the legend the inversion method (Method 1) is indicated by “i” and solid lines, and the conversion method (Method 2) is indicated by “c” and by dash-dotted lines. The use of CSR is indicated by light blue and blue lines, and the GFZ by light red and red lines. Each of the small dispersion graphics shows the time series obtained with inversion versus conversion methods (purple square), and the use of CSR versus GFZ data set (green dots). For each of these couple of time series the value of their regression index m (as in Eq. 2) is indicated in square parentheses. In the pannel **(c)**, the vertical axis indicate the basin (number, the region (EA, WA, AP) and area in 10^6 km^2) in descending order from the largest. For each basin, monthly differences are plotted for the two methods (purple) and for the two datasets (green). The light colors represent the (quadratic sum of) the monthly difference with respect to (the average of) the monthly errors. The normal colors represent the difference in regression index (m as in Eq. 2) and the gray bar is the error on the trend same of Fig. 8d and Fig. 9d. All these quantity are normalized with respect to the trend.

Variability of mass changes

V. R. Barletta et al.

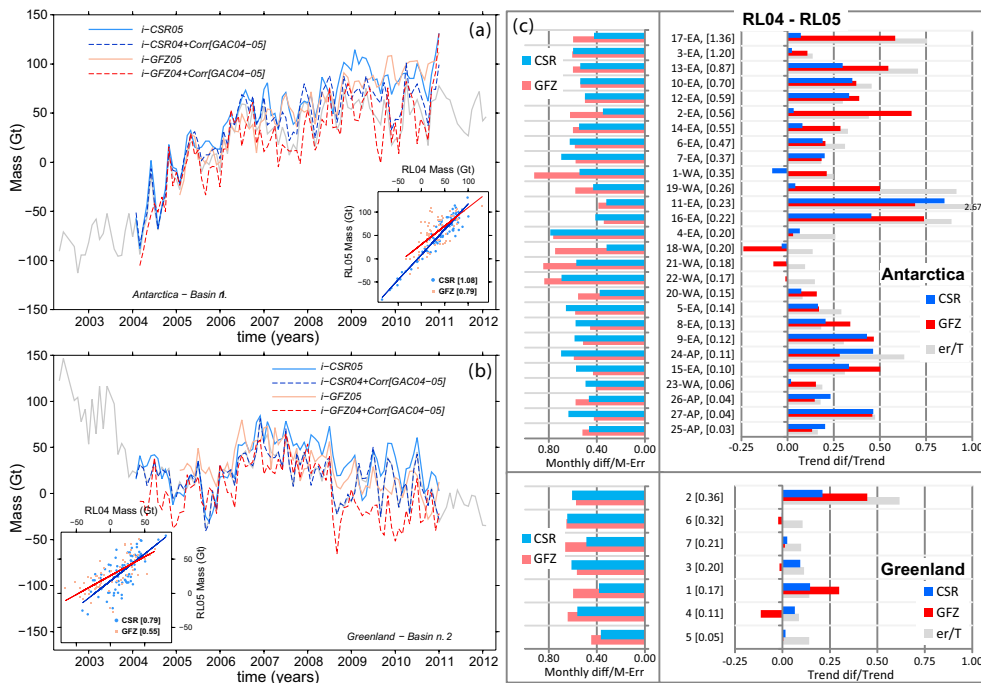


Fig. 5. Monthly solution for basin 1 for Antarctica (a) and basin 2 for Greenland (b). Comparison between the two releases RL04 and RL05 (CSR and GFZ) with inversion method: the use of CSR is indicated by light blue and blue lines, and the GFZ by light red and red lines. The release RL05 is the solid line, while the RL04, with GAC[04–05] correction, is the dashed line. The grey line represent the original CSR time series before the GAC correction. Each of the small dispersion graphics shows the time series obtained with RL04 versus RL05 with the use of CSR (blue) and GFZ (red). In the panel (c), for each basin monthly differences between RL04 and RL05 are plotted for the use of CSR (blue) and GFZ (red). The light colors represent the (quadratic sum of) the monthly difference with respect to (the average of) the monthly errors. The normal colors represent the difference in regression index (m as in Eq. 2) and the gray bar is the error on the trend same of Figs. 8d and 9d. All these quantity are normalized with respect to the trend.

Title Page

Abstract Introduction

Conclusions References

Tables Figures

◀ ▶

◀ ▶

Back Close

Full Screen / Esc

Printer-friendly Version

Interactive Discussion



Variability of mass changes

V. R. Barletta et al.

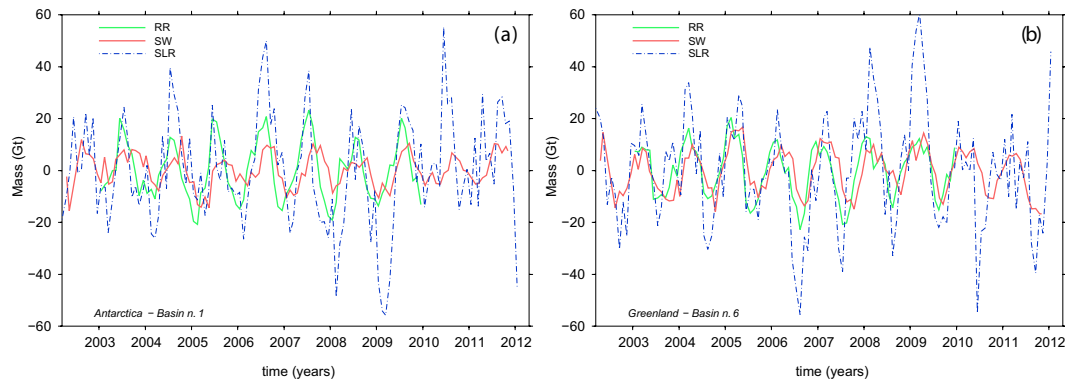


Fig. 6. Three time series de-trended correction in Gt for degree one, for basin 1 for Antarctica **(a)** and basin 6 for Greenland **(b)**. The green line (RR) use the Rietbroek et al. (2012a), the red line (SW) use the (Swenson et al., 2008) and the blue dotted line use the SLR – Cheng et al. (2010) geocenter contribution to the selected basin.

Title Page

Abstract

Introduction

Conclusions

References

Tables

Figures

◀

▶

◀

▶

Back

Close

Full Screen / Esc

Printer-friendly Version

Interactive Discussion



Variability of mass changes

V. R. Barletta et al.

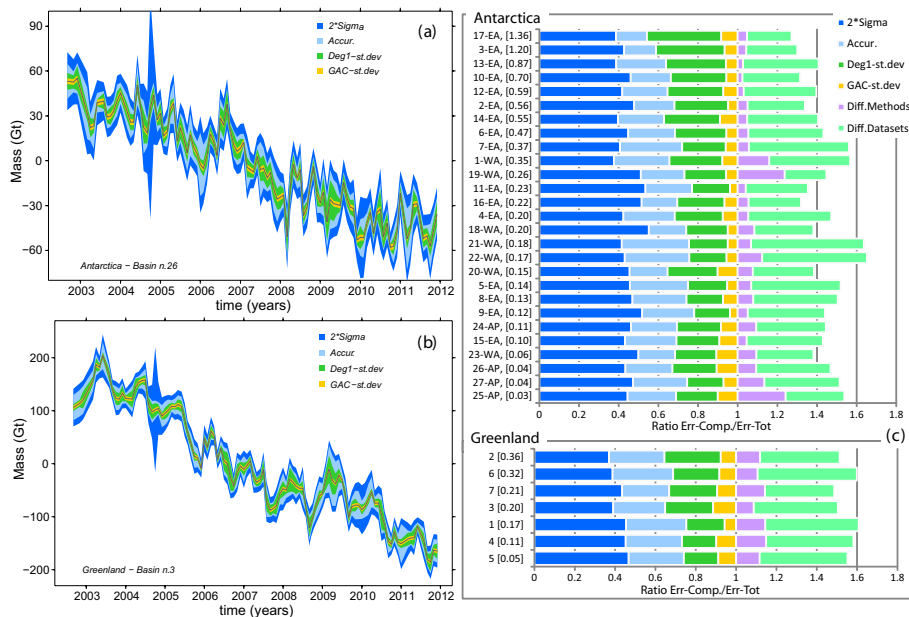


Fig. 7. Monthly average solution for basin 26, Antarctic Peninsula **(a)** and basin 3 for Greenland **(b)**. Each color in the band around the average represents a contribution to the error estimate: the blue is the 2sigma propagated from the data calibrated errors, the light blu is the accuracy error computed as described in Sect. 3.5, the green is the standard deviation for the degree-1 component, and the yellow is the standard deviation computed for the GAC correction as the grey band shown in Fig. 1. In the panel **(c)**, the same colors are used to refer to the same component, but for each basin here the average (over the whole time series) of the component is plotted with respect to the average of total error. The light purple and light green bars (one on top of the other) represent the same quantity of Fig. 4 in light colors bars (light purple and light green, one beside the other).

Title Page

Abstract

Introduction

Conclusions

References

Tables

Figures

◀

▶

◀

▶

Back

Close

Full Screen / Esc

Printer-friendly Version

Interactive Discussion



Variability of mass changes

V. R. Barletta et al.

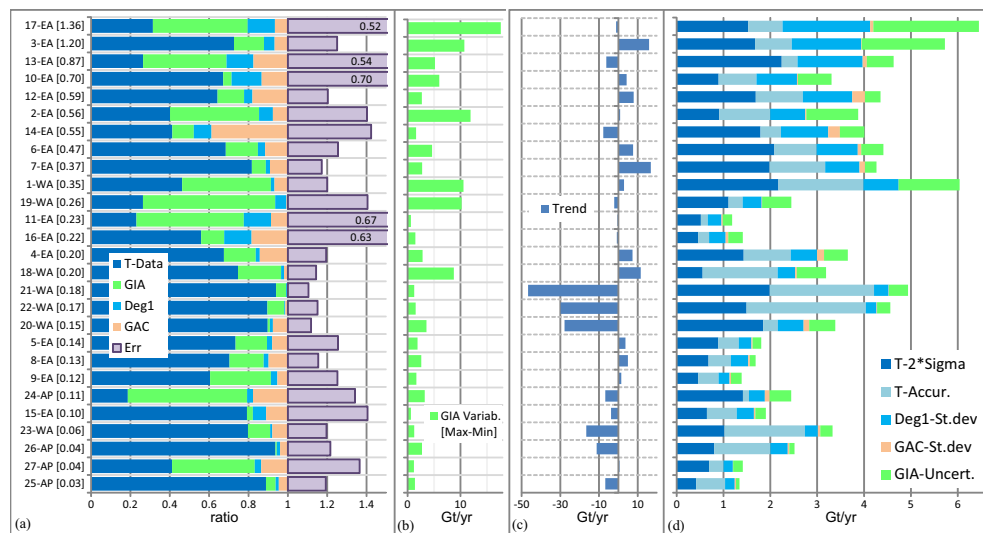


Fig. 8. Trend summary for Antarctica. The labels for vertical axis on the left are the same for the 4 panels and indicate the basin as in Fig. 4. Panel (a) shows each relative contribution to the trend, the Data (blue), GIA (Green), Deg-1 (sky blue) and GAC (light orange). The relative Errors (violet) is shown on top of the trend bar. Panel (b) shows the GIA variability (in Gt yr^{-1}) as the difference between the maximum and the minimum values for GIA corrections among the four different models used. Panel (c) shows the total trend in Gt yr^{-1} for the average time series. Panel (d) shows the total error (in Gt yr^{-1}) on the trend as sum of each of its component: 2sigma from the trend computation (blue), the trend accuracy error (light blue), the standard deviation (st. dev.) for the trend on degree-1 (sky blue), the GAC st. dev (light orange) and the GIA uncertainties (green) as max on GIA uncertainties among all models.

[Title Page](#)
[Abstract](#)
[Introduction](#)
[Conclusions](#)
[References](#)
[Tables](#)
[Figures](#)
[◀](#)
[▶](#)
[◀](#)
[▶](#)
[Back](#)
[Close](#)
[Full Screen / Esc](#)
[Printer-friendly Version](#)
[Interactive Discussion](#)


Variability of mass changes

V. R. Barletta et al.

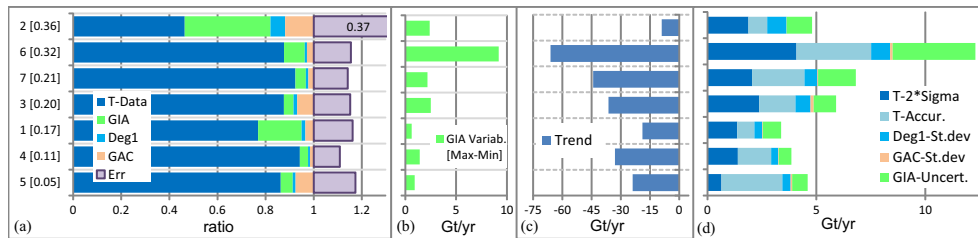


Fig. 9. Trend summary for Greenland with same meaning of Fig. 8.

Title Page

Abstract Introduction

Conclusions References

Tables Figures

◀ ▶

◀ ▶

Back Close

Full Screen / Esc

Printer-friendly Version

Interactive Discussion



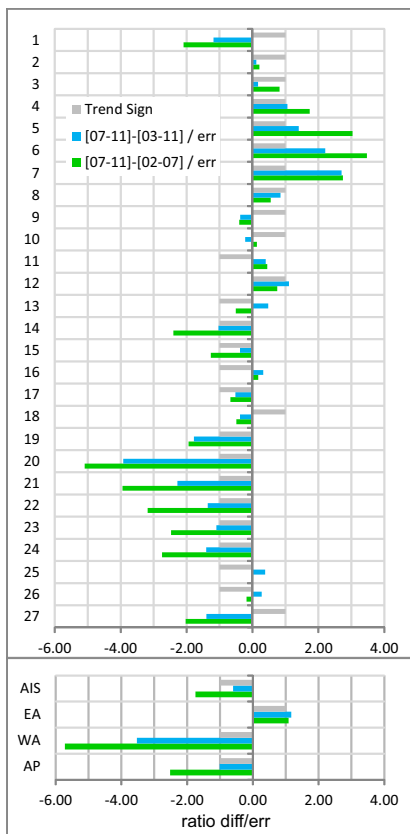


Fig. 10. Acceleration summary for Antarctica. The green bars represents the difference between the trends of two periods with respect to the error: trends for August 2007–November 2011 minus trends for August 2002–July 2007. The sky-blue bars represents the difference, with respect to the error, between the trends in the last period and the whole period of GRACE: trends for August 2007–November 2011 minus trends for January 2003–November 2011. The grey bars represents the sign of the trend in the period January 2003–November 2011. The increment (or decrement) ratio is significant if it has an absolute value greater than one.

Variability of mass changes

V. R. Barletta et al.

Title Page

Abstract Introduction

Conclusions References

Tables Figures

◀ ▶

◀ ▶

Back Close

Full Screen / Esc

Printer-friendly Version

Interactive Discussion



Variability of mass changes

V. R. Barletta et al.

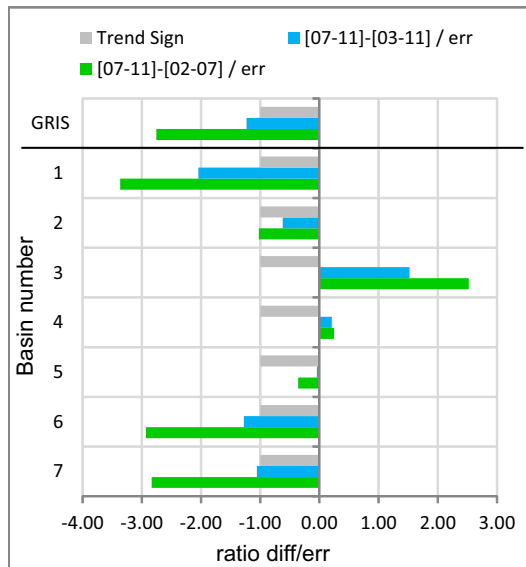


Fig. 11. Acceleration summary for Greenland. The same as in Fig. 11.

Title Page

Abstract Introduction

Conclusions References

Tables Figures

◀ ▶

◀ ▶

Back Close

Full Screen / Esc

Printer-friendly Version

Interactive Discussion

